A 12 year observation of water-soluble ions in TSP aerosols collected at a remote marine location in the western North Pacific: an outflow region of Asian dust

S.K.R. Boreddy[1] and Kimitaka Kawamura[1*]

[1]Institute of Low Temperature Science, Hokkaido University, N19, W8, Kita-ku, Sapporo 060-0819, Japan.

[*]Corresponding author
Kimitaka Kawamura,
Institute of Low Temperature Science,
Hokkaido University,
Sapporo 060-0819, Japan.
E-mail: kawamura@lowtem.hokudai.ac.jp

Abstract:

In order to characterize the long term trend of remote marine aerosols, a 12-year observation was conducted for water-soluble ions in TSP aerosols collected from 2001-2012 in the Asian outflow region at a Chichijima Island in the western North Pacific. We found a clear difference in chemical composition between the continentally affected and marine background air masses over the observation site. Asian continental air masses are delivered from late autumn to spring, whereas marine air masses were dominated in summer. Concentrations of nss-SO_4^{2-}, NO_3^-, NH_4^+, nss-K^+ and nss-Ca^{2+} are high in winter and spring and low in summer. On the other hand, MSA^- exhibits higher concentrations during spring and winter, probably due to springtime dust bloom or due to the direct continental transport of MSA^- to the observation site. We couldn't find any clear decadal trend for Na^+, Cl^-, Mg^{2+} and nss-Ca^{2+} in all seasons, although there exists a clear seasonal trend. However, concentrations of nss-SO_4^{2-} continuously decreased from 2007-2012, probably due to the decreased SO_2 emissions in East Asia especially in China. In contrast, nss-K^+ and MSA^- concentrations continuously increased from 2001-2012 during winter and spring seasons, demonstrating that biomass burning and/or terrestrial biological emissions in East Asia are increasingly more transported from the Asian continent to the western North Pacific. This study also demonstrates that Asian dusts can act as an important source of nutrients for phytoplankton and thus sea-to-air emission of DMS over the western North Pacific.

Key words: Water-soluble inorganic ions, long-range atmospheric transport, Asian dust, western North Pacific, springtime bloom.

1 Introduction

The atmosphere is mostly composed of gases, but also contains suspended liquid and solid particles, called aerosols. Knowledge of the physical and chemical properties of aerosols is important, because of their role in atmospheric processes and climate change. Marine aerosols perturb the earth's radiation balance directly by scattering and absorbing the incoming solar radiation or indirectly by acting as cloud condensation nuclei (CCN) and thus altering their water uptake properties (Twomey, 1977; Charlson et al., 1991; Ramanathan et al., 2001). The strength of these direct and indirect effects depends on the concentration, size distribution, and chemical composition of the atmospheric aerosols (Coakley et al., 1983). In addition, marine aerosols play an important role in atmospheric sulphur cycle of the marine portion (O'Dowd et al., 1997; Faloona, 2009). Thus, meticulous information on the chemical and physical properties of marine aerosol is crucial for the aerosol studies.

Sea salt, ubiquitous and major component in the marine total suspended particulate (TSP) mass has been recognized as the dominant contributor to the clear-sky albedo over the oceans (Haywood et al., 1999). Sea salt aerosols are produced at the ocean surface through the bubble bursting mechanism (Woodcock, 1953). They can affect the chemical and microphysical properties of other aerosol components by taking up and releasing chemically reactive compounds including sulfur and halogen compounds. The sea salt concentration primarily depends on wind speed ranging from 2 to 100 μgm^{-3} (Fitzgerald, 1991). Additionally sea salt aerosol particles are hygroscopic by nature (Tang et al., 1997) and hence act as CCN (O'Dowd et al., 1999; Quinn et al., 2000; Ayash et al., 2008).

Non-sea salt (nss-) SO_4^{2-} acts effectively as a reflector of solar radiation and as CCN and, therefore, controls the cloud microphysical properties and cloud albedo (Charlson et al., 1987). The principal source of nss-SO_4^{2-} in the marine atmosphere is the oxidation of gaseous dimethyl sulphide (DMS) emitted by marine phytoplankton (Charlson et al., 1987). Graf et al. (1997) reported that the global burden of nss-SO_4^{2-} (0.78 Tg sulpher) is distributed 37% from fossil fuel burning, 36% from volcanoes, 25% from marine DMS, and 1.6% from biomass burning. On the other hand, continental anthropogenic nss-SO_4^{2-} and nitrate (NO_3^-) are transported over the remote marine locations and perturb the marine background conditions (Duce and Tindale, 1991; Uematsu et al., 1992; Matsumoto et al., 1998). Methanesulfonate (MSA) is also derived by the oxidation of DMS that originates from the biological activity in the ocean/land (Uematsu et al., 1992; Pavuluri et al., 2011; Miyazaki et al., 2012; Kunwar and Kawamura, 2014).

Anthropogenic and mineral aerosols have significant impact on global climate and also influence the atmospheric chemistry as well as marine ecosystems in remote oceanic regions (Matsumoto et al., 2004). Bridgman (1990) reported that on average about 185–483 x 10^6 ton global aerosols per year are caused by anthropogenic sources including transportation, stationary combustion, industrial process, solid waste disposal and other miscellaneous sources. East Asia is one of the most swiftly developing regions in the world and consumes a significant amount of fossil fuels leading to an apparent increase in anthropogenic emission of gaseous pollutants and particulate matter. In addition, high dust loading in spring time is another discernible feature of air quality over the East Asian region (Sun et al., 2001). The long-range atmospheric transport of anthropogenic and mineral aerosols from the Asian continent to the North Pacific (Kawamura et al., 2003; Matsumoto et al., 2004) and sometimes even North America (Jaffe et al., 2003) by the westerlies may have significant impacts on global radiation balance, atmospheric chemistry, and ocean biogeochemistry (Satheesh and Moorthy, 2005; Rudich et al., 2002; Jickells et al., 2005; Houghton, 2001).

Chichijima Island, a remote marine site in the western North Pacific, is located on the lee side of a large industrial area and, therefore, this site is well suitable for the study of long-range transport of air pollutants in East Asia and also the perturbation of anthropogenic activity in the remote marine atmosphere. However, the observational data on aerosol chemistry over the western North Pacific are very sparse (Kawamura et al., 2003; Mochida et al., 2003; Matsumoto et al., 2004; Mochida et al., 2010; Chen et al., 2013; Boreddy et al., 2014). There is no study on the long term observations of ionic chemical species from the western North Pacific. In order to investigate the annual and seasonal behavior of water-soluble inorganic ions and to clarify decadal trend of the long-range transport of continental aerosols to the remote ocean area, we carried out measurements of atmospheric aerosols at a Chichijima in the western North Pacific.

2 Experimental

2.1 Sampling site and aerosol sampling

Figure 1 shows the sampling location of Chichijima Island in the western North Pacific and its surrounding East Asian regions. This island is about 1000 km from the main Japanese Main Island, Honshu and 2000 km away from the Asian continent. The area within 40 km of this station is covered by oceans and seas. The population of Chichijima is about 2,300 and the island's area about 24 km^2 according to the report of the Tokyo metropolitan

government bureau of general affairs (http://www.soumu.metro.tokyo.jp/07ogasawara/28.html, accessed in November 2011). The observatory is not affected by local pollution, but by the long-range transport of polluted air from the Asian Continent during winter and spring. Therefore the observations at Chichijima Island are useful in discussing the long-range transport of polluted air on a regional scale.

Total suspended particles (TSP) were collected on a weekly basis at the Satellite Tracking Centre of Japan Aerospace Exploration Agency (JAXA, elevation: 254 m) in Chichijima Island (27°04′N; 142°13′E) at a height of 5 m above ground level during 2001-2012. Aerosol particles were collected on precombusted (450°C, 3 hours) quartz filters (20 x 25 cm, Pallflex 2500QAT-UP) using a high volume air sampler with a flow rate of 1 m^3 min^{-1} (Kawamura et al., 2003). Filters were placed in a clean glass jar with a Teflon-lined screw cap during the transport and storage. After the sampling, the filters were recovered into the glass jar and stored in a freezer room at - 20°C prior to analysis.

2.2 Analysis of chemical species

All samples were analyzed at Institute of Low Temperature Science, Hokkaido University, Japan. The procedure of chemical analysis is as follows: A punch of 20 mm in diameter from each filter sample was extracted with 10 mL organic-free ultrapure water (resistivity of >18.2 MΩ cm, Sartorius arium 611 UV) and ultrasonicated for 30 min. These extracts were the filtrated through a disk filter (Millex-GV, 0.22 μm pore size, Millipore) to remove filter debris and particles and were analyzed for major inorganic ions (MSA^-, Cl^-, SO_4^{2-}, NO_3^-, Na^+, NH_4^+, K^+, Ca^{2+}, and Mg^{2+}) using an ion chromatograph (761 Compact IC, Metrohm, Switzerland).

Major anions were separated on a SI-90 4E Shodex column (Showa Denko, Tokyo, Japan) using a mixture of 1.8 mM Na_2CO_3 + 1.7 mM $NaHCO_3$ solution at a flow rate of 1.2 mL min^{-1} as an eluent and 40 mM H_2SO_4 for a suppressor. For cation measurements, a Metrosep C2-150 (Metrohm) column was used by using a mixture of 4 mM tartaric acid ($C_4H_6O_6$) + 1 mM dipicolinic acid ($C_7H_5NO_4$) solution as eluent at a flow rate of 1.0 mL min^{-1}. The injection loop volume was 200 μL. A calibration curve was evaluated using authentic standards along with a sequence of filter samples. The analytical error in duplicate analysis was about 10 %. Contributions from the field blanks varied between 0.004-0.132 ppm and 0.002-0.013 ppm for anions and cations, respectively, during the sampling period. The concentrations of all inorganic ions reported here are corrected for field blanks that were collected during the sampling period (2001-2012). Total 545 samples were used in this study.

151

152 **2.3 Synoptic wind pattern and general meteorology**

153 Figure 2 shows monthly mean wind vectors at 850 mb pressure level over Chichijima
154 Island and its surrounding regions, as obtained from the National Centers for Environmental
155 Prediction (NCEP)/National Centre for Atmospheric Research (NCAR) reanalysis
156 (http://www.esrl.noaa.gov/psd/data/gridded/reanalysis/), have been used to ascertain the
157 synoptic conditions during the study period 2001-2012. It is very clear that, from January to
158 April the synoptic winds are stronger, circulation is westerly (from the Asian Continent to the
159 Pacific) and the observation site experiences long-range continental aerosols (anthropogenic
160 and dust). The winds are weakening by May/June and the wind direction changes to south-
161 easterly and continue until August/September. The observation site gets pristine marine air
162 masses, low wind speed and also much rainfall during south-easterly regime. Again the wind
163 starts shifting from south-easterly to north-westerly/westerly by October and becomes
164 stronger towards December and January-April again. Therefore, on the basis of major
165 synoptic meteorological conditions as above, a year is divided into four seasons: winter
166 (December- February), spring (March-May), summer (June-August) and autumn (September-
167 November) over Chichijima Island.

168 Based on the historical records from 1974 to 2011 (see Figure S1 in supporting
169 information) (http://weatherspark.com/averages/33165/Chichijima-Chichi-Shima-Chubu-
170 Japan), the temperature typically varies from 16°C-30°C and is rarely below 13°C or above
171 31°C over the course of a year. In summer, with an average daily high temperature above
172 28°C whereas in winter average daily high temperature below 22°C. The relative humidity
173 typically ranges from 55% (winter) to 94% (summer) over the year, rarely dropping below
174 45% and reaching as high as 98%. The highest average wind speed of 4 m/s occurs in spring,
175 when the average daily maximum wind speed is 6 m/s. The lowest average wind speed of 2
176 m/s occurs in summer, when the average daily maximum wind speed is 4 m/s. In this region,
177 westerly winds dominate in winter to spring and trade winds dominate in summer to autumn.

178

179 **2.4 Backward air mass trajectories**

180 Figure 3 shows daily 10-day backward air mass trajectories arriving over the
181 observation site, Chichijima at 500 m above the ground level, which were computed for each
182 month using the HYSPLIT model, developed by NOAA/ARL
183 (http://ready.arl.noaa.gov/HYSPLIT.php) (Draxler and Rolph, 2003) during the study period
184 of 2001-2012. The selection of 500m altitude for air mass trajectories was due to the potential

impact of the air-sea surface interactions within the boundary layer (Zielinski et al., 2014; Rozwadowska at al., 2010). The sampling site Chichijima is in the western North Pacific located in the outflow region of Asian dusts and polluted air masses from China. At 500 m altitude, all trajectories come from the East Asian countries during winter and spring. Therefore, based on the sampling point (JAXA, 254m) and source regions, we assumed that 500m is the minimum suitable altitude to calculate backward air mass trajectories over Chichijima Island. As we discussed above, during winter and spring months, the air masses originate from Siberia passing over Northeast Asia, whereas in the summer months they mostly originate from the Pacific, where pristine air masses exist.

2.5 Evaluation of non sea salt analysis

The contributions from other sources excluding sea salts are calculated using Na^+ as a sea spray marker. However, in this study, for better accuracy, non sea salt components were evaluated from the seasalt (ss) Na^+ fraction [*Bowen*, 1979; *Becagli et al*., 2005].

$$nss\text{-}SO_4^{2-} = [SO_4^{2-}] - 0.253 * ss\text{-}Na^+ \quad (1)$$

$$nss\text{-}Ca^{2+} = [Ca^{2+}] - 0.038 * ss\text{-}Na^+ \quad (2)$$

$$nss\text{-}K^+ = [K^+] - 0.037 * ss\text{-}Na^+ \quad (3)$$

where $[SO_4^{2-}]$, $[Ca^{2+}]$ and $[K^+]$ are the total measured TSP mass concentrations and $ss\text{-}Na^+$ was calculated using the four equation system reported below and knowing total Na^+, total Ca^{2+}, the mean Ca^{2+}/Na^+ ratio in the crust ($(Na^+/Ca^{2+})_{crust}$ = 1.78 w/w; Bowen, 1979) and the mean Ca^{2+}/Na^+ ratio in sea water ($(Ca^{2+}/Na^+)_{seawater}$ = 0.038 w/w; Bowen, 1979).

$$\left.\begin{aligned} ss\text{-}Na^+ &= Na^+ - nss\text{-}Na^+ \\ nss\text{-}Na^+ &= nss\text{-}Ca^{2+} * (Na^+/Ca^{2+})_{crust} \\ nss\text{-}Ca^{2+} &= Ca^{2+} - ss\text{-}Ca^{2+} \\ ss\text{-}Ca^{2+} &= ss\text{-}Na^+ * (Ca^{2+}/Na^+)_{seawater} \end{aligned}\right\} \quad (4)$$

Crustal contribution to water-soluble sodium ranged from 0.004-0.94 with a mean of 0.078±0.071 during the study period.

3 Results and Discussion

3.1 Ion balance

In order to assess the quality of the analysis, we performed an ion balance calculation using major anions (Cl^-, SO_4^{2-}, NO_3^-) and cations (Na^+, NH_4^+, K^+, Ca^{2+}, and Mg^{2+}) assuming

that most of the ions are in the solutions. Based on the electro neutrality principle, the sum of total anions (μeq m^{-3}) should be equal to the sum of total cations (μeq m^{-3}) in the solutions and this ratio is a good indicator to study the acidity of aerosols over the sampling site. The following equations are used here to calculate the charge balance between cations and anions.

$$\text{Cation equivalent } (\Sigma^{+}) = \frac{Na^{+}}{23} + \frac{NH_4^{+}}{18} + \frac{K^{+}}{39} + \frac{Mg^{2+}}{12} + \frac{Ca^{2+}}{20} \quad (5)$$

$$\text{Anion equivalents } (\Sigma^{-}) = \frac{SO_4^{2-}}{48} + \frac{NO_3^{-}}{62} + \frac{Cl^{-}}{35.5} \quad (6)$$

The relationship between anions and cations for different seasons are shown in Figure 4. We found that correlation coefficients of anions vs. cations were higher than 0.92 for all seasons, which represent a good quality of data and also indicate that ions share a common origin (Zhang et al., 2011). The slopes of linear regression lines for the seasonally stratified data are >1 with the following order: summer (1.264) > spring (1.256) >autumn (1.252) > winter (1.231). This result suggests that in all seasons, the TSP was apparently acidic. As most of the major ions were measured except for hydrogen ions (H^{+}), the cation deficits are probably due to H^{+} ion.

3.2 Temporal variations of major inorganic species, MSA^{-}/nss-SO_4^{2-} and Σ^{+}/Σ^{-} ratios

Figure 5 presents temporal variations of major water-soluble ionic species, MSA^{-}/nss-SO_4^{2-} and Σ^{+}/Σ^{-} ratios for the period 2001-2012 over the sampling site. All the measured ions showed a clear temporal trend for each year during the study period. The Σ^{+}/Σ^{-} ratio (μeq m^{-3}), which is a good indicator of acidity of aerosols over the environment, ranged from 0.8 to 1.6 with a mean of 1.2±0.1, demonstrating that aerosol particles are acidic over Chichijima Island (Figure 5a). The MSA^{-}/nss-SO_4^{2-}, which can be used as a tracer to assess the contribution of biogenic sources to sulfate in the atmosphere (Savoie and Prospero, 1989), varied between 0.002 and 0.064 with a mean of 0.014±0.01 and summertime maxima (Figure 5b).

Sea salt species (Cl^{-} and Na^{+}) are found as the most abundant ranging from 0.92 to 16.6 μg m^{-3} with a mean of 6.31±2.61 μg m^{-3} and from 0.61 to 7.36 μg m^{-3} with a mean of 3.39±1.20 μg m^{-3}, respectively (see Figure 5i and 5k). Concentrations of nss-SO_4^{2-} varied from 0.09 to 7.85 μg m^{-3} with a mean of 2.17±1.53 μg m^{-3} (see Figure 5e) whereas those of nitrate ranged from 0.09 to 1.17 μg m^{-3} (mean 0.57±0.37 μg m^{-3}). Although NH_4^{+} was less abundant throughout the sampling period, we found significant levels under the influence of continental air masses in the spring. Its concentrations ranged from 0.01 to 1.10 μg $m^{-3}$with a

mean of 0.17±0.16 μg m^{-3} (Figure 5h). Concentrations of MSA^-, a marker of biogenic source, varied from 0.006 to 0.055 μg m^{-3} with a mean of 0.021±0.009 (Figure 5f). Nss-Ca^{2+} (nss-K^+), a tracer for dust (biomass burning), ranged from 0.002 to 0.84 μg m^{-3} (0.002 to 0.19 μg m^{-3}) with a mean of 0.13±0.15 μg m^{-3} (0.04±0.03 μg m^{-3}) (Figure 5c, 5d). Concentrations of Mg^{2+} ranged from 0.06 to 0.78 μg m^{-3} with a mean of 0.40±0.14 μg m^{-3} (Figure 5j). It is also noteworthy that the sum of all the water-soluble inorganic ions (WSIM) ranged from 2.9 to 25.7 μg m^{-3} with a mean of 13.1±4.8 μg m^{-3} in Chichijima TSP aerosols for the study period of 2001-2012 (not shown as a figure).

3.3 Monthly variations of major chemical species and MSA^-/nss-SO_4^{2-}

Figure 6 gives Box-Whisker diagrams of monthly variations of different chemical species at Chichijima Island in the western North Pacific for the period of 2001-2012. Almost all the ions showed a clear monthly/seasonal variation with higher concentrations during the long-range atmospheric transport of continental air mass and lower concentrations under the influence of marine air mass. Monthly or seasonally averaged concentrations of major ions (mean±SD) during 2001-2012 at Chichijima Island in the western North Pacific are reported in Table 1. The presence of monthly averaged trend is demonstrated by Theil-Sen Slope test (Sen, 1968; Theil, 1950). The results show that these differences are statistically significant with Theil-Sen slope values of less than 0.01.

As illustrated in Figure 6a and b, sea salt particles are characterized by a gradual increase from autumn to winter, with a peak in early spring (March). Thereafter, Na^+, Cl^- minimized in early summer (June) and again increased toward winter. We found the significantly high concentration during August; probably due to the influence of Southeast Asian air masses (see Figure 3). This trend of sea salts is similar to that of wind speed over the sampling site; that is, higher wind speeds during spring/winter and lower in the summer. This result suggests that the concentrations of sea salts are mainly depend on wind speed. It is also worthy to note that the similar seasonal pattern can also be seen in the concentrations of Mg^{2+} (see Figure 6c), indicating that Mg^{2+} comes from the ocean rather continental sources. This is further supported by the existing correlation between Mg^{2+} and Na^+. We found a strong correlation (R^2= 0.94 and slope= 0.117) between Mg^{2+} and Na^+ with the ratio being very close to seawater (0.12).

The seasonal variations of NH_4^+ and NO_3^- are characterized by spring maxima and summer minima. NH_4^+ concentrations are low throughout the sampling period over the Chichijima Island (Figure 6d, e), probably because the sampling site is far away from the

source regions of ammonia over the Asian continent (Boreddy et al., 2014; Matsumoto et al., 2007). The residence time of NH_3 is around several hours in the marine boundary layer (Quinn et al., 1990) and the concentration of NH_3 transported from continental to remote marine locations should be considerably low. Interestingly, we found a significantly higher concentration of NO_3^- than that of NH_4^+ over the sampling site, which may result from some additional NO_3^- sources. The heterogeneous reaction, $HNO_3 + NaCl \rightarrow NaNO_3$, can provide an additional source of NO_3^- in TSP aerosols (Wu et al., 2006) over the observation site. Further, the low temperature over East Asian regions in winter and spring would favor the shift from the gas phase of nitric acid to nitrate in the particle phase, which could lead to higher concentration of NO_3^- that is transported to the western North Pacific in winter and spring. On the other hand, nss-K^+ that is derived mainly from biomass burning was also quite low in Chichijima TSP aerosols, although it shows a higher concentration in winter and spring than in summer and autumn. The seasonal variation of nss-SO_4^{2-} showed maxima in the spring/winter and minima in summer (see Figure 6h), being similar to that of NO_3^-. This result indicates that the higher levels of nss-K^+ during the winter and spring mainly associated with the long-range atmospheric transport of anthropogenic/biomass burning particles over the observation site.

The concentrations of nss-Ca^{2+} drastically increased in spring when the Asian dusts were transported over the observation site by westerly winds (see Figure 6i). This result is consistent with the previous studies (Kawamura et al., 2003; Suzuki et al., 2008; Guo et al., 2011) where nss-Ca^{2+} maximized in spring. A strong seasonal variability was found in MSA^- concentrations with higher values in spring followed by winter and lower values in autumn and summer. This strong seasonal variability in MSA^- can be ascribed to seasonality of photochemistry, biology, and meteorology. It is worth noting that the mass concentration of MSA^- showed similar seasonal variation with nss-Ca^{2+} and NO_3^-, although its concentrations are much lower than that of nss-Ca^{2+} and NO_3^-. This result suggests that there should be a link between dust and biological emissions and NO_3 radicals (see Figure 6g). This point will be discussed in more details in the subsequent sections. The mass ratio MSA^-/nss-SO_4^{2-} showed a clear, distinct variation characterized by a gradual increase from winter to spring with a peak in summer. It again gradually decreased toward winter (see Figure 6f). This result illustrates that the contribution of marine biogenic sources to nss-SO_4^{2-} was higher in summer, because of higher solar radiation that enhances the biological activity over the sampling site. We also found co-variation between MSA^-/nss-SO_4^{2-} ratio and air temperature, both of which showed maxima in summer followed by spring and minima in winter.

3.4 Annual variations of different chemical species on a seasonal scale

Annual mean concentrations of major ions (mean±SD) for different seasons during 2001-2012 are reported in Table 2. The presence of annual averages trend is demonstrated by Mann-Kendall test, results were also reported in Table 2. The Mann–Kendall trend test (Mann, 1945; Kendall, 1975) is one of the widely used non-parametric tests to detect significant trends in time series. In this test, the absolute value of Z is compared to the standard normal cumulative distribution to define if there is a trend or not at the selected level α (=0.01, in this study) of significance. A positive (negative) value of Z indicates an upward (downward) trend.

Figure 7 presents the annual variations of selected chemical species for different seasons in the period of 2001-2012. Although there exist some seasonal trends of ions, we couldn't find any clear annual trends for the species Cl^-, Mg^{2+} and nss-Ca^{2+} in all seasons. However, nss-SO_4^{2-} and NO_3^- showed a clear annual trend for all seasons, with an increase from 2001-2004 and decrease from 2007-2012. Lu et al. (2010) reported that total SO_2 emission in China increased by 53% (21.7-33.2 Tg, at an annual growth rate of 7.3%) from 2000 to 2006, during which emissions from power plants are the main sources of SO_2 in China with an increase from 10.6 to 18.6 Tg per year. Geographically, emission from north China increased by 85%, whereas that from the south increased by only 28%. The growth rate of SO_2 emission slowed down around 2005, and began to decrease after 2006 mainly due to the wide operation of flue-gas desulfurization (FGD) devices in power plants in response to a new policy of Chinese government. This change in the SO_2 emissions was exactly recorded in our observation at Chichijima in the western North Pacific, that is, the decreasing trend of SO_4^{2-} concentrations over the observation site can be explained by the decrease in SO_2 emissions in China after 2006. Further, these results are supported by the annual variation of nss-SO_4^{2-}/Na^+ and nss-NO_3^-/Na^+ mass ratios (see Figure 7j and k). The nss-SO_4^{2-}/Na^+ ratio showed a clear annual trend in winter and spring with an increase from 2001 to 2004 and decreasing trend from 2007 to 2012. Therefore, nss-SO_4^{2-} concentrations in the western North Pacific are gradually decreasing, because of the suppressed emission of SO_2 over East Asia, especially in China.

In contrast, the annual variation of nss-K^+ showed an increasing trend from 2001 to 2004 and 2006 to 2012, suggesting that biomass burning emissions in East Asia are continuously increasing and transported to the western North Pacific by long-range

atmospheric transport. This result is further supported by the study of Verma et al. (2015), who reported long term measurements of biomass burning organic tracers (levoglucosan, mannosan and galactosan) for the period of 2001-2013 over the same observation site, Chichijima Island. They found a continuous increase in the concentrations of biomass burning tracers from 2006 to 2013, which is mainly caused by enhanced biomass burning in East Asia. It is of interest to note that the annual variation of MSA^- concentrations have shown a gradual increase from 2001 to 2012 during the winter and spring seasons, indicating that direct transport of MSA^- from the continental surface to the remote marine locations is continuously increasing. On the other hand, NH_4^+ concentrations showed a gradual decrease from 2006 to 2012 during winter and spring seasons, whereas in summer and autumn, we couldn't find any clear annual trends in the abundance of NH_4^+.

3.5 Correlation analyses among the inorganic ions

In order to find the crucial information about sources of ions, we performed a correlation analysis among the ions for different seasons (see Table 1) because the ion concentrations emitted from the same source or similar reaction pathway should show a good correlation between them. Tables 1a, b, c, and d show the results of correlation analyses of major ions for winter, spring, summer, and autumn respectively during the study period. In all seasons, we found strong correlation (excellent correlation during summer and autumn) among Na^+, Mg^{2+}, and Cl^- indicating that these ions have similar source and mainly come from sea spray. Although NH_4^+ concentrations are low throughout the sampling period, it shows good correlation with SO_4^{2-} during all seasons.

During winter, nss-K^+, a tracer of biomass burning source, strongly correlates with nss-SO_4^{2-} whereas NO_3^-, a tracer of anthropogenic source, correlates with NH_4^+, Na^+, and nss-K^+ with a relatively strong correlation coefficient ($r > 0.55$), suggesting that they are derived from biomass burning and anthropogenic sources in the Asian continent, respectively. In spring, Ca^{2+} shows relatively strong correlation with NO_3^- ($r=0.62$) and moderately correlated with Mg^{2+}, nss-K^+, and nss-SO_4^{2-} indicating that they are derived from similar sources or reaction pathways. It is important to note that Na^+ moderately correlated with acetic ions (NO_3^- and SO_4^{2-}) during spring, whereas no correlation in summer reveals that chloride loss is prominent in spring than in summer and also tells that NH_3 and HNO_3 probably react with sea salt particles in the marine atmosphere.

3.6 Percent contribution of major ions to total WSIM

386 The percent contributions of individual inorganic species to the total WSIM are
387 shown as a pie chart in Figure 8 for the different seasons. Among all the inorganic species,
388 sea salt (NaCl) is a major contributor to the WSIM, followed by nss-SO_4^{2-} and NO_3^- during all
389 seasons. Na^+ and Cl^- together contributed ~ 70%, 66%, 80% and 82% to the total WSIM for
390 winter, spring, summer and autumn, respectively, whereas nss-SO_4^{2-} contributed ~ 26%,
391 24%, 11% and 10%, respectively. The nss-Ca^{2+} shows a significant contribution (about 2%)
392 to WSIM in spring, indicating a long-range atmospheric transport of Asian dusts over the
393 observation site. Similarly, Mg^{2+} contributed to the total WSIM by about 3% in all seasons.
394 We found a significant depletion of chloride during winter and spring, probably due to
395 the atmospheric mixing of anthropogenic pollutants such as SO_2, NO_3, etc. (Boreddy et al.,
396 2014a). Figure 9a and b show the monthly and seasonal variations of Cl^-/Na^+ mass ratio
397 during the study period. The monthly-averaged Cl^-/Na^+ ratio varied from 1.58 to 2.05 with a
398 mean value of 1.79±0.15. Although the mean mass ratio is almost equal to that of seawater
399 (1.8), we found significant chlorine loss in the winter and spring samples. Atmospheric
400 processing of anthropogenic pollutants/minerals and their mixing with sea salt particles
401 during the long-range atmospheric transport are probably responsible for the chlorine loss.
402 On the other hand acid displacement also plays an important role in chloride depletion over
403 the marine environment through the following reactions,
404
405 $2NaCl + H_2SO_4 \rightarrow Na_2SO_4 + 2HCl$ (5)
406 $NaCl + HNO_3 \rightarrow NaNO_3 + HCl$ (6)
407
408 Further, Mochida et al. (2003) reported high abundance of oxalic acid in the
409 Chichijima TSP aerosols in spring. Oxalic acid may be internally mixed with dust-derived
410 minerals. Previous studies of Asian dust showed that oxalate was largely mixed with dust
411 particles (Sullivan and Prather, 2007). Therefore, it is reasonable to assume that the spring
412 time chlorine loss over the western North Pacific was most likely due to the displacement of
413 Cl^- with oxalate through the following reaction,
414
415 $2NaCl + H_2C_2O_4 \rightarrow Na_2C_2O_4 + 2HCl$ (7)
416
417 In contrast, during the summer and autumn, we found an excess of chloride over the
418 observation site, because of some additional source of chloride added to the TSP aerosols.

In order to investigate which acids are responsible for the depletion of chloride, we performed regression analysis between the Cl^-/Na^+ mass ratio and acidic species, nss-SO_4^{2-}, NO_3^-, MSA^- and oxalic acid for different seasons during 2001-2012 as shown in Figure 10. The regression analysis was verified by *t*-test. The results show that the differences between Cl^-/Na^+ mass ratio and acidic species are statistically significant with two tailed P value is ≤ 0.001 for each season during the study period. For all seasons, nss-SO_4^{2-} moderately correlated with Cl^-/Na^+ mass ratios with negative correlation coefficients (R^2) of 0.38, 0.29, 0.35 and 0.45 for winter, spring, summer, and autumn, respectively, whereas NO_3^- moderately correlated during winter (R^2= -0.30), weakly correlated in autumn (R^2= -0.22) and has no correlation in spring and summer. These results suggest that sulfate has more responsibility for the chloride depletion than nitrate.

On the other hand, the biogenic tracer, MSA^-, moderately correlated during summer (R^2= -0.29) and has weak correlation in winter and spring. Freshly emitted MSA and H_2SO_4 (from oceanic biological productivity associated with the upwelling of nutrient rich water) are also little contribute to the chloride depletion by coating with sea salts, especially in summer. Interestingly, during spring, the Cl^-/Na^+ mass ratio did not correlate with NO_3^-, MSA^- but weakly correlated with nss-SO_4^{2-}. These results suggest that some other organic acids, such as oxalic acid (because of its high abundance during spring), are responsible for the chloride depletion during spring. in fact, we found that oxalic acid significantly correlate with the chlorine loss in winter (-0.30), spring (-0.28) and autumn (-0.36) (see Figure 10d). These results confirm that oxalic acid plays an important role in a chlorine loss.

3.7 Which biological source is more important as a contributor to MSA^- ?

To better identify which biological source as a more significant contribution to MSA^-, we compared the monthly mean variation of MSA^- with chlorophyll *a* (Chl. *a* (mg/m3), a satellite derived biogenic tracer) during the study period as shown in Figure 11. Chl. *a* concentrations were downloaded from MODIS AQUA satellite over the region of 140˚E-145˚E, 25˚N-30˚N for the period July 2002-December 2012. We found a clear monthly/seasonal variation in Chl. *a* concentration, which gradually increased from autumn to early spring and then decreased from mid spring to summer. Surprisingly, similar seasonal pattern can also be seen in the concentrations of nss-Ca^{2+} (see Figure 6i), indicating that there should exist a possible link between the long-range transport of Asian dusts (or a springtime bloom) and the ocean productivity in the western North Pacific. The production of algal blooms may quickly respond to dust deposition (nutrients) over the surface ocean (Gabric et

al., 2004). By changing the phytoplankton productivity, dusts can act as important source of DMS production (Jickells et al., 2005). However, the mechanisms of marine phytoplankton response to a dust input from the atmosphere are still facing with numerous uncertainties, a subject of scientific discussion.

Ramos et al. (2005) observed the massive Saharan dust storms along with algal bloom observed in the north Atlantic in August 2004. Bishop et al. (2002) observed an increase in chlorophyll *a* over a couple of weeks in the North Pacific after passage of Gobi desert dust cloud. Springtime bloom in the north East China Sea and Japan Sea was observed by TOMS and SeaWiFS satellites to be initiated one month earlier than usual, being correlated with an Asian dust event in association with precipitation. Such event leads to a supply of bioavailable iron and to induce a deepening of the critical depth, which results in an early initiation of the bloom (Jo et al., 2007). On the other hand, Gabric et al. (2004) revealed that the dust storms in Australia (2002-2003) lead to advection of large dust plumes over the Southern Ocean, and observed a coherence between optical characteristics of the Southern Ocean atmosphere and dust loading by satellite and field data on surface ocean chlorophyll *a*. Therefore, it is noteworthy that the transported atmospheric dust particles can act as a fertilizer to stimulate the production of microscopic marine plants (plankton/algae blooms).

As discussed in section 3.3, the monthly variation of MSA^- gradually increased from winter to spring, with a peak in April and gradually decreased towards summer and autumn months. Interestingly, MSA^- maximized in April whereas Chlorophyll *a* maximized in March, although both are tracers for the marine biological activity. It is also important to mention that the highest concentration of MSA^- was observed one month after the Asian dust deposition over the ocean surface, suggesting that there may be a time lag between the dust deposition and DMS emissions. Therefore, we assume that there are two possible sources for higher MSA^- concentrations in winter/spring over the Chichijima island; (1) direct transport of MSA^- from the continental sources, such as industrial emissions (Lu et al., 2010), terrestrial higher plants (Pavuluri et al., 2013), and forest floors (Miyazaki et al., 2012), and (2) springtime bloom of phytoplankton over the western North Pacific.

Another factor that could affect MSA concentrations is concentrations of NO_3 radicals, which are among the key oxidants for MSA production. Polluted air mass with higher NO_x concentrations gives higher MSA yields relative to SO_2 from DMS oxidation (Yin et al., 1990). Under prevailing westerly polluted winds, significant amount of anthropogenic NO_x can be transported from East Asia over the western North Pacific, which could enhance the MSA concentrations relative to the less polluted pristine air masses.

Similar results are reported elsewhere (Yin et al., 1990; Jensen et al., 1991; Mihalopoulos et al., 1992; Gao et al., 1996). Further, temperature is also an important factor to control the MSA^- concentrations through the mechanism of DMS oxidation by hydroxyl radicals (Arimoto et al., 1996). In the present study, we found lower concentrations of MSA^- during summer and autumn months when ambient temperature is higher, demonstrating that lower temperature may lead to higher MSA concentration in this region. However, the MSA concentrations in the marine atmosphere could be affected by multiple processes relating to primary productivity, such as spatial variability of phytoplankton species, air-sea exchange rates of DMS, and different oxidation pathways of DMS. In addition, variations in environmental conditions such as temperatures, precipitation patterns, sea-ice conditions, winds and ocean currents could also control the concentrations of MSA (Gao et al., 1996).

To further clarify the relations between MSA^- and nss-Ca^{2+}, we examined the intense Ca episodes during the study period (March 2002), which can be related with variations in MSA^- as shown in Figure 12 as a typical example. Figure12a shows the SeaWiFS (Sea-viewing Wide Field-of-view Sensor, flying aboard Orbview-2) images, which captured the large Asian dust storms over the North Pacific during March 17-April 2, 2002. Dust storms originate in the deserts of North China and Mongolia. The East Asian dust storm appears to have diminished somewhat on March 20, 2002, as compared to previous days. However, there seemed a new batch of dust rising toward the left side of this image. This scene spans from eastern Asia across Japan and over the western North Pacific, where the dust was partly entrained by a low-pressure system.

On the other hand, possible variations of MSA^- concentrations related to the East Asian dusts are shown in Figure 11b. Interestingly, we found higher levels of MSA^- after the Asian dust deposition over the ocean surface. This evidence strongly reveals that Ca episodes supply the nutrients to significantly stimulate plankton blooms accompanied by statistically significant variations in MSA concentrations in the atmosphere few days after the episodes. This result also demonstrates that Asian dusts can act as an important source of macro and micro nutrients including iron for phytoplankton and thus sea-air emission of DMS over the western North Pacific.

3.8 Comparison of major inorganic ions over the Pacific

The mean concentrations of NO_3^-, nss-SO_4^{2-}, and MSA^- at Chichijima during the period 2001-2012 are compared those from several other remote marine sites in the Pacific as summarized in Table 4. Results from the Chichijima data show that mean NO_3^- and nss-SO_4^{2-}

are higher than those from other remote marine locations. The mean concentration of nitrate (0.58 μgm^{-3}) at Chichijima is more than 4 times higher than those from other remote marine sites (Fanning, Nauru, Funafuti, American Samoa, Rarotonga, and N. Caledonia) and more than twice higher than those from Midway. Whereas concentrations of nss-sulfate at Chichijima (2.12 μgm^{-3}) is 4 times higher than at Fanning, Midway, and N. Caledonia and more than 7 times higher than those from American Samoa and Norfolk. The mean concentration of MSA^- (0.02 μgm^{-3}) at Chichijima is comparable to those from other remote marine locations (see Table 4). These results suggest a similarity to that of the oceanic biological productivity in the North Pacific.

In contrast, the mean MSA^- concentration at Fanning in the equatorial Pacific is about twice higher (0.044 μgm^{-3}) than that of Chichijima. Savoie and Prospero (1989) have found high biological productivity associated with the upwelling of nutrient rich water near the equatorial divergence with mean DMS levels of 3.8 nmol/l in the surface ocean. They also documented that in the oligotrophic regions, the mean concentrations of MSA in the air and DMS in the sea water vary over the narrow range from 0.02-0.03 μgm^{-3} and 1.4-1.7 nmol/l, respectively.

The mean concentration ratio ($MSA^-/nss\text{-}SO_4^{2-}$) at Chichijima is 0.02, which is lower than those of other remote marine locations by a factor of 5-7, indicating a substantial impact from continentally derived sulfate. At the tropical stations, American Samoa and Fanning Island, MSA and $nss\text{-}SO_4^{2-}$ ratios exhibit similar values with mean ratios of 0.07 and 0.06, respectively, indicating a cleanest locations regarding to the continental inputs (Arimoto et al., 1987). This result further supports our assumption that Asian dusts can act as an important source of nutrients that stimulate DMS production in the ocean surface followed the emission to the marine atmosphere over the western North Pacific. However, it is rather less important that yield of MSA from DMS oxidation is enhanced as a function of temperature (Hyens et al., 1986).

4 Summary and Conclusions

We conducted 12-year observation of water-soluble inorganic ions in TSP aerosols, from the remote marine location, Chichijima Island, in the western North Pacific. Long-term observation of marine aerosols provides the following findings.

1. Water-soluble inorganic ions in the TSP aerosols are dominated by sea salt particles (Na^+ and Cl^-), which contributed about 75% to the total WSIM followed by anthropogenic species such as $nss\text{-}SO_4^{2-}$, and NO_3^-.

2. Sea salt components showed prominent peaks in autumn and winter months and minimized in spring and summer probably due to the variations in wind speed over the observation site. nss-SO_4^{2-}, NO_3^-, and nss-K^+ showed higher concentrations in winter and spring, due to the atmospheric long-range transport of anthropogenic pollutants and biomass burning emissions in East Asia. Although NH_4^+ concentrations are relatively low throughout the sampling period over the Chichijima Island, they showed prominent peaks in spring and winter months. The concentrations of nss-Ca^{2+} in TSP drastically increased in spring when the Asian dusts are delivered to the observation site.
3. Interestingly, concentrations of nss-SO_4^{2-} during winter and spring decreased from 2007 to 2012 probably due to the decrease in SO_2 emissions in China after 2006. A similar trend was seen in the concentrations of NO_3^- during the study period. In contrast, the concentration of nss-K^+ showed continuous increase from 2001 to 2004 and 2006 to 2012, suggesting that biomass burning emissions in East Asia are more increased followed by the atmospheric transport to the western North Pacific. On the other hand, MSA^- concentrations during winter to spring continuously increased from 2001 to 2012, indicating that direct continental transport of Asian dust followed by springtime bloom in the ocean play an important role on the annual variation of MSA^- concentrations over the western North Pacific.
4. We also found there is a time lag between the measured concentration of MSA^- in the aerosols and satellite derived biological tracer (Chlorophyll *a*), suggesting that variability of phytoplankton, sea-air exchange rate of DMS emissions, and other environmental conditions can play an important role in controlling the concentrations of MSA^- over the observation site.

This study provides a long-term record (2001-2012) of water-soluble species in TSP aerosols on Chichijima Island in the western North Pacific and focuses on the impact of long-range transport of Asian dusts and anthropogenic pollutants from East Asia on the distributions of water-soluble ionic species. This impact has changed suddenly over the last decade and becoming a challenge to the future climate effects of Asian aerosols over the western North Pacific. We believe that this study has further implications regarding the radiative forcing and climate models over the oceanic regions.

Acknowledgement

This study was in part supported by the Japan Society for the Promotion of Science (grant-in-aid 1920405 and 24221001). We appreciate the financial support of a JSPS

589 fellowship to S. K. R. Boreddy. The authors gratefully acknowledge the NOAA Air
590 Resources Laboratory for the provision of the HYSPLIT transport dispersion model from the
591 website http://www.arl.noaa.gov/ready/hysplit4.html. We are grateful to NCEP/NCAR for
592 their reanalysis provided by NOAA-CIRES Climate Diagnostic Center, Boulder, Colorado
593 from their website (http://www.cdc.noaa.gov), which was used in this study.
594

595 **References**

596 Arimoto, R., Duce, R. A., Ray, B. J., Hewitt, A. D., and Williams, J. J.: Trace elements in the
597 atmosphere of American Samoa: Concentrations and deposition to the tropical South
598 Pacific, Journal of Geophysical Research, 92, 8465-8479, 1987.
599 Arimoto, R., Duce, R. A., Savoie, D. L., Prospero, J. M., Talbot, R., Cullen, J. D., Tomza, U.,
600 Lewis, N. F., and Ray, B. J.: Relationships among aerosol constituents from Asia and
601 the North Pacific during PEM-West A, Journal of Geophysical Research: Atmospheres,
602 101, 2011-2023, 10.1029/95JD01071, 1996.
603 Ayash, T., Gong, S., and Jia, C. Q.: Direct and indirect shortwave radiative effects of sea salt
604 aerosols, Journal of Climate, 21, 3207-3220, 2008.
605 Bishop, J. K. B., Davis, R. E., and Sherman, J. T.: Robotic observations of dust storm
606 enhancement of carbon biomass in the North Pacific, Science, 298, 817-821, 2002.
607 Boreddy, S. K. R., Kawamura, K., and Jung, J. S.: Hygroscopic properties of particles
608 nebulized from water extracts of aerosols collected at Chichijima Island in the western
609 North Pacific: An outflow region of Asian dust, J Geophys Res-Atmos, 119, 167-178,
610 Doi 10.1002/2013jd020626, 2014.
611 Bridgman, H. A.: Global Air Pollution: Problems for the 1990s, Belhaven Press, 25Floral
612 Street, London WCzzz2E, 9DS., 1990.
613 Charlson, R. J., Lovelock, J. E., Andreae, M. O., and Warren, S. G.: Oceanic phytoplankton,
614 atmospheric sulphur, cloud albedo and climate, Nature, 326, 655-661, 1987.
615 Charlson, R. J., Langner, J., Rodhe, H., Leovy, C. B., and Warren, S. G.: Perturbation of the
616 Northern-Hemisphere Radiative Balance by Backscattering from Anthropogenic
617 Sulfate Aerosols, Tellus A, 43, 152-163, 1991.
618 Chen, J., Kawamura, K., Liu, C.-Q., and Fu, P.: Long-term observations of saccharides in
619 remote marine aerosols from the western North Pacific: A comparison between 1990–

1993 and 2006–2009 periods, Atmospheric Environment, 67, 448-458, http://dx.doi.org/10.1016/j.atmosenv.2012.11.014, 2013.

Coakley, J. A., Cess, R. D., and Yurevich, F. B.: The Effect of Tropospheric Aerosols on the Earths Radiation Budget - a Parameterization for Climate Models, J Atmos Sci, 40, 116-138, 1983.

Draxler, R. R., and Rolph, G. D.: HYSPLIT (HYbrid Single-Particle Lagrangian Integrated Trajectory) Model access via NOAA ARL READY Website (http://www.arl.noaa.gov/ready/hysplit4.html). NOAA Air Resources Laboratory, Silver Spring, MD, 2003.

Duce, R. A., and Tindale, N. W.: Atmospheric Transport of Iron and Its Deposition in the Ocean, Limnology and Oceanography, 36, 1715-1726, 1991.

Faloona, I.: Sulfur processing in the marine atmospheric boundary layer: A review and critical assessment of modeling uncertainties, Atmospheric Environment, 43, 2841–2854, 2009.

Fitzgerald, J. W.: MARINE AEROSOLS - A REVIEW, Atmospheric Environment Part a-General Topics, 25, 533-545, 1991.

Gabric, A. J., Simo, R., Cropp, R. A., Hirst, A. C., and Dachs, J.: Modeling estimates of the global emission of dimethylsulfide under enhanced greenhouse conditions (vol 18, art no GB2014, 2004), Global Biogeochemical Cycles, 18, 2004.

Gao, Y., Arimoto, R., Duce, R. A., Chen, L. Q., Zhou, M. Y., and Gu, D. Y.: Atmospheric non-sea-salt sulfate, nitrate and methanesulfonate over the China Sea, Journal of Geophysical Research: Atmospheres, 101, 12601-12611, 10.1029/96JD00866, 1996.

Graf, H. F., Feichter, J., and Langmann, B.: Volcanic sulfur emissions: Estimates of source strength and its contribution to the global sulfate distribution, J Geophys Res-Atmos, 102, 10727-10738, 1997.

Guo, Y.-t., Zhang, J., Wang, S.-g., She, F., and Li, X.: Long-term characterization of major water-soluble inorganic ions in PM10 in coastal site on the Japan Sea, J Atmos Chem, 68, 299-316, 10.1007/s10874-012-9223-8, 2011.

Haywood, J. M., Ramaswamy, V., and Soden, B. J.: Tropospheric aerosol climate forcing in clear-sky satellite observations over the oceans, Science, 283, 1299-1303, 1999.

Houghton, J. T., Ding, Y., Griggs, D.J., Noguer, M., van der Linden, P.J., Dai, X., Maskell, K., Johnson, C.A.: Climate Change 2001: the Scientific Basis., Cambridge University Press, Cambridge, 2001.

653 Hynes, A. J., Wine, P. H., and Semmes, D. H.: Kinetics and mechanism of OH reactions with
654 organic sulfides, J. Phys. Chem., 90, 4148-4156, 1986.
655 Jaffe, D., McKendry, I., Anderson, T., and Price, H.: Six 'new' episodes of trans-Pacific
656 transport of air pollutants, Atmospheric Environment, 37, 391-404,
657 http://dx.doi.org/10.1016/S1352-2310(02)00862-2, 2003.
658 Jensen, N. R., Hjorth, J., Lohse, C., Skov, H., and Restelli, G.: Products and mechanism of
659 the reaction between NO3 and dimethylsulphide in air, Atmospheric Environment. Part
660 A. General Topics, 25, 1897-1904, http://dx.doi.org/10.1016/0960-1686(91)90272-9,
661 1991.
662 Jickells, T. D., An, Z. S., Andersen, K. K., Baker, A. R., Bergametti, G., Brooks, N., Cao, J.
663 J., Boyd, P. W., Duce, R. A., Hunter, K. A., Kawahata, H., Kubilay, N., laRoche, J.,
664 Liss, P. S., Mahowald, N., Prospero, J. M., Ridgwell, A. J., Tegen, I., and Torres, R.:
665 Global Iron Connections Between Desert Dust, Ocean Biogeochemistry, and Climate,
666 Science, 308, 67-71, 10.1126/science.1105959, 2005.
667 Jo, C. O., Lee, J. Y., Park, K. A., Kim, Y. H., and Kim, K. R.: Asian dust initiated early
668 spring bloom in the northern East/Japan Sea, Geophysical Research Letters, 34, 2007.
669 Kawamura, K., Ishimura, Y., and Yamazaki, K.: Four years' observations of terrestrial lipid
670 class compounds in marine aerosols from the western North Pacific, Global
671 Biogeochemical Cycles, 17, 1003, 10.1029/2001GB001810, 2003.
672 Kendall, M. G.: Rank Correlation Methods, Griffin, London, 1975.
673 Kunwar, B., and Kawamura, K.: One-year observations of carbonaceous and nitrogenous
674 components and major ions in the aerosols from subtropical Okinawa Island, an
675 outflow region of Asian dusts, Atmos. Chem. Phys., 14, 1819-1836, 10.5194/acp-14-
676 1819-2014, 2014.
677 Lu, Z., Streets, D. G., Zhang, Q., Wang, S., Carmichael, G. R., Cheng, Y. F., Wei, C., Chin,
678 M., Diehl, T., and Tan, Q.: Sulfur dioxide emissions in China and sulfur trends in East
679 Asia since 2000, Atmos. Chem. Phys., 10, 6311-6331, 10.5194/acp-10-6311-2010,
680 2010.
681 Mann, H. B.: Nonparametric tests against trend, Econometrica, 13, 245–259, 1945.
682 Matsumoto, Uyama, Y., Hayano, T., and Uematsu, M.: Transport and chemical
683 transformation of anthropogenic and mineral aerosol in the marine boundary layer over
684 the western North Pacific Ocean, Journal of Geophysical Research: Atmospheres, 109,
685 D21206, 10.1029/2004JD004696, 2004.

686 Matsumoto, K., Nagao, I., Tanaka, H., Miyaji, H., Iida, T., and Ikebe, Y.: Seasonal
687 characteristics of organic and inorganic species and their size distributions in
688 atmospheric aerosols over the northwest Pacific Ocean, Atmospheric Environment, 32,
689 1931-1946, 1998.
690 Matsumoto, K., Minami, H., Hayano, T., Uyama, Y., Tanimoto, H., and Uematsu, M.:
691 Regional climatology of particulate carbonaceous substances in the northern area of the
692 east Asian Pacific rim, Journal of Geophysical Research: Atmospheres, 112, D24203,
693 10.1029/2007JD008607, 2007.
694 Miyazaki, Y., Fu, P. Q., Kawamura, K., Mizoguchi, Y., and Yamanoi, K.: Seasonal variations
695 of stable carbon isotopic composition and biogenic tracer compounds of water-soluble
696 organic aerosols in a deciduous forest, Atmos. Chem. Phys., 12, 1367-1376,
697 10.5194/acp-12-1367-2012, 2012.
698 Mochida, M., Kawabata, A., Kawamura, K., Hatsushika, H., and Yamazaki, K.: Seasonal
699 variation and origins of dicarboxylic acids in the marine atmosphere over the western
700 North Pacific, J. Geophys. Res., [Atmos], 108, D6, 4193,
701 doi:4110.1029/2002JD002355, 2003.
702 Mochida, M., Kawamura, K., Fu, P., and Takemura, T.: Seasonal variation of levoglucosan in
703 aerosols over the western North Pacific and its assessment as a biomass-burning tracer,
704 Atmospheric Environment, 44, 3511-3518,
705 http://dx.doi.org/10.1016/j.atmosenv.2010.06.017, 2010.
706 Mihalopoulos, N., Nguyen, B. C., Boissard, C., Campin, J. M., Putaud, J. P., Belviso, S.,
707 Barnes, I., and Becker, K. H.: Field study of dimethylsulfide oxidation in the boundary
708 layer: Variations of dimethylsulfide, methanesulfonic acid, sulfur dioxide, non-sea-salt
709 sulfate and aitken nuclei at a coastal site, J Atmos Chem, 14, 459-477,
710 10.1007/BF00115251, 1992.
711 O'Dowd, C. D., Smith, M. H., Consterdine, I. E., and Lowe, J. A.: Marine aerosol, sea-salt,
712 and the marine sulphur cycle: A short review, Atmos. Environ., 31, 73-80, 1997.
713 O'Dowd, C. D., Lowe, J. A., and Smith, M. H.: Coupling sea-salt and sulphate interactions
714 and its impact on cloud droplet concentration predictions, Geophysical Research
715 Letters, 26, 1311-1314, 1999.
716 Pavuluri, C. M., Kawamura, K., Aggarwal, S. G., and Swaminathan, T.: Characteristics,
717 seasonality and sources of carbonaceous and ionic components in the tropical aerosols
718 from Indian region, Atmos Chem Phys, 11, 8215-8230, 2011.

719 Prospero, J. M., and Savoie, D. L.: Long-term of nss-sulfate and nitrate in aerosols on
720 Midway Island, 1981-2000: Evidence of increased (now decreasing?) anthropogenic
721 emissions from Asia, Journal of Geophysical Research, Vol 108, NO. D1,
722 doi:10.1029/2001JD001524, 2003.
723 Pavuluri, C. M., Kawamura, K., Mihalopoulos, N., and Fu, P.: Year-round observations of
724 water-soluble ionic species and trace metals in Sapporo aerosols: implication for
725 significant contributions from terrestrial biological sources in Northeast Asia, Atmos.
726 Chem. Phys. Discuss., 13, 6589-6629, 10.5194/acpd-13-6589-2013, 2013.
727 Quinn, P. K., Bates, T. S., Johnson, J. E., Covert, D. S., and Charlson, R. J.: Interactions
728 between the sulfur and reduced nitrogen cycles over the central Pacific Ocean, Journal
729 of Geophysical Research: Atmospheres, 95, 16405-16416, 10.1029/JD095iD10p16405,
730 1990.
731 Quinn, P. K., Bates, T. S., Coffman, D. J., Miller, T. L., Johnson, J. E., Covert, D. S., Putaud,
732 J. P., Neususs, C., and Novakov, T.: A comparison of aerosol chemical and optical
733 properties from the 1st and 2nd Aerosol Characterization Experiments, Tellus Series B-
734 Chemical and Physical Meteorology, 52, 239-257, 2000.
735 Ramanathan, V., Crutzen, P. J., Kiehl, J. T., and Rosenfeld, D.: Aerosols, climate, and the
736 hydrological cycle, Science, 294, 2119-2124, 2001.
737 Ramos, A. G., Martel, A., Codd, G. A., Soler, E., Coca, J., Redondo, A., Morrison, L. F.,
738 Metcalf, J. S., Ojeda, A., Suarez, S., and Petit, M.: Bloom of the marine diazotrophic
739 cyanobacterium Trichodesmium erythraeum in the Northwest African upwelling, Mar
740 Ecol Prog Ser, 301, 303-305, 2005.
741 Rudich, Y., Khersonsky, O., and Rosenfeld, D.: Treating clouds with a grain of salt,
742 Geophysical Research Letters, 29, 2064, 10.1029/2002GL016055, 2002.
743 Satheesh, S. K., and Krishna Moorthy, K.: Radiative effects of natural aerosols: A review,
744 Atmospheric Environment, 39, 2089-2110,
745 http://dx.doi.org/10.1016/j.atmosenv.2004.12.029, 2005.
746 Savoie, D. L., Prospero, J. M., and Saltzman, E. S.: Non sea salt sulfate and nitrate in trade
747 wind aerosols at Barbodos: Evidence for long-range transport, Journal of Geophysical
748 Research, Vol. 94,NO. D4, 5069-5080, 1989.
749 Savoie, D. L., and Prospero, J. M.: Comparison of oceanic and continental sources of non-
750 sea-salt sulphate over the Pacific Ocean, Nature, 339, 685-687, 1989.
751 Sen, P. K.: Estimates of the regression coefficient based on Kendall's tau", Journal of the
752 American Statistical Association **63**: 1379–1389, 1968.

753 Sullivan, R. C., and Prather, K. A.: Investigations of the Diurnal Cycle and Mixing State of
754 Oxalic Acid in Individual Particles in Asian Aerosol Outflow, Environ Sci Technol, 41,
755 8062-8069, 10.1021/es071134g, 2007.
756 Sun, J., Zhang, M., and Liu, T.: Spatial and temporal characteristics of dust storms in China
757 and its surrounding regions, 1960–1999: Relations to source area and climate, Journal
758 of Geophysical Research: Atmospheres, 106, 10325-10333, 10.1029/2000JD900665,
759 2001.
760 Suzuki, I., Hayashi, K., Igarashi, Y., Takahashi, H., Sawa, Y., Ogura, N., Akagi, T., and
761 Dokiya, Y.: Seasonal variation of water-soluble ion species in the atmospheric aerosols
762 at the summit of Mt. Fuji, Atmospheric Environment, 42, 8027-8035,
763 http://dx.doi.org/10.1016/j.atmosenv.2008.06.014, 2008.
764 Tang et al.: Thermodynamics and optical properties of sea salt aerosols, Journal of
765 Geophysical Research, 102, 23269-23275, 1997.
766 Theil, H.:A rank-invariant method of linear and polynomial regression analysis, 1,2, and 3:
767 Ned. Akad. Wentsch Proc., 53:386-392, 521-525, and 1397-1412, 1950.
768 Twomey, S.: Influence of Pollution on Shortwave Albedo of Clouds, J Atmos Sci, 34, 1149-
769 1152, 1977.
770 Uematsu, M., Sugita, T., Anikiev, V. V., and Medvedev, A. N.: Large-scale transport of
771 pollution aerosol over the east coast of Asia, Geophysical Research Letters, 19, 2219-
772 2221, 10.1029/92GL02639, 1992.
773 Verma, S. K., Kawamura, K., Chem, J., Fu, P., and Zhu, C.: Thirteen years of observations
774 on biomass burning organic tracers over Chichijima Island in the western North Pacific:
775 an outflow region of Asian Aerosols, doi: 10.1002/2014JD022224, 2015.
776 Woodcock: Salt nuclei in marine air as a function of attitude and wind force, Journal of
777 meterology, 10, 362-371, 1953.
778 Wu, D., Tie, X., and Deng, X.: Chemical characterizations of soluble aerosols in southern
779 China, Chemosphere, 64, 749-757,
780 http://dx.doi.org/10.1016/j.chemosphere.2005.11.066, 2006.
781 Yin, F., Grosjean, D., Flagan, R., and Seinfeld, J.: Photooxidation of dimethyl sulfide and
782 dimethyl disulfide. II: Mechanism evaluation, J Atmos Chem, 11, 365-399,
783 10.1007/BF00053781, 1990.
784 Zhang, T., Cao, J. J., Tie, X. X., Shen, Z. X., Liu, S. X., Ding, H., Han, Y. M., Wang, G. H.,
785 Ho, K. F., Qiang, J., and Li, W. T.: Water-soluble ions in atmospheric aerosols

measured in Xi'an, China: Seasonal variations and sources, Atmos Res, 102, 110-119, http://dx.doi.org/10.1016/j.atmosres.2011.06.014, 2011.

Table 1. Seasonal mean concentrations of major water-soluble ions (mean ± standard deviation) and the Theil-Sen slope value for the seasonal trend during the period 2001-2012 at Chichijima Island in the western North Pacific.

	MSA^-	Cl^-	NO_3^-	nss-SO_4^{2-}	Na^+	NH_4^+	nss-K^+	nss-Ca^{2+}	Mg^{2+}
Winter	0.02±0.00	7.10±0.88	0.78±0.14	3.06±0.43	4.12±0.47	0.19±0.06	0.05±0.03	0.12±0.03	0.48±0.05
Spring	0.03±0.01	6.18±1.20	0.84±0.15	2.97±0.89	3.32±0.59	0.23±0.10	0.05±0.02	0.30±0.12	0.42±0.07
Summer	0.02±0.00	4.94±1.54	0.24±0.09	1.06±0.59	2.52±0.71	0.11±0.13	0.02±0.01	0.04±0.04	0.29±0.09
Autumn	0.01±0.00	7.12±2.61	0.43±0.11	1.31±0.42	3.62±1.06	0.11±0.05	0.05±0.04	0.04±0.03	0.40±0.11
Theil-Sen Slope (2001-2012)									
Slope	0	-0.0067	-0.0004	-0.0045	-0.0048	-0.0002	0.0005	0	-0.0005

Table 2. Annual mean concentrations of major inorganic ions (mean ± standard deviation) and the Mann-Kendall test for annual trend during 2001-2012 at Chichijima Island in the western North Pacific.

	MSA^-	Cl^-	NO_3^-	nss-SO_4^{2-}	Na^+	NH_4^+	nss-K^+	nss-Ca^{2+}	Mg^{2+}
2001	0.01±0.00	5.65±2.82	0.47±0.29	1.67±1.11	2.87±1.36	0.09±0.04	0.03±0.01	0.15±0.19	0.33±0.16
2002	0.02±0.01	6.84±2.66	0.61±0.41	2.81±1.66	3.59±1.20	0.27±0.17	0.05±0.03	0.18±0.26	0.44±0.15
2003	0.02±0.01	7.23±2.16	0.60±0.36	2.17±1.21	3.85±1.19	0.13±0.07	0.05±0.03	0.10±0.11	0.45±0.15
2004	0.02±0.01	8.41±4.14	0.54±0.39	2.27±1.65	4.46±1.42	0.16±0.07	0.06±0.04	0.08±0.08	0.50±0.16
2005	0.02±0.00	7.25±2.24	0.69±0.40	2.32±1.24	4.12±1.03	0.10±0.07	0.04±0.01	0.11±0.10	0.46±0.13
2006	0.02±0.01	6.58±2.56	0.64±0.43	2.20±1.56	3.58±1.07	0.14±0.15	0.03±0.03	0.16±0.23	0.41±0.14
2007	0.02±0.01	5.63±1.51	0.67±0.35	2.77±1.39	3.36±1.01	0.36±0.32	0.07±0.04	0.17±0.15	0.39±0.13
2008	0.02±0.01	4.83±2.35	0.49±0.29	2.28±1.42	2.89±1.12	0.16±0.11	0.08±0.06	0.08±0.09	0.33±0.13
2009	0.03±0.01	6.46±2.64	0.57±0.37	1.51±1.18	3.47±1.03	0.13±0.08	0.03±0.02	0.09±0.08	0.40±0.11
2010	0.02±0.01	5.15±2.31	0.55±0.38	1.71±1.19	2.71±1.25	0.15±0.14	0.03±0.02	0.15±0.20	0.32±0.15
2011	0.02±0.01	5.56±1.51	0.51±0.31	1.67±1.34	2.85±0.81	0.14±0.15	0.03±0.04	0.10±0.13	0.34±0.11
2012	0.02±0.01	7.04±1.87	0.64±0.51	2.03±1.43	3.49±0.97	0.18±0.18	0.04±0.02	0.15±0.15	0.43±0.12
Mean	0.02±0.00	6.39±1.04	0.58±0.07	2.12±0.42	3.44±0.54	0.17±0.07	0.05±0.01	0.13±0.03	0.40±0.05
Mann-Kendall Nonparametric Test (2001-2012)									
Z value	2.34**	-1.71	-1.56	-2.49**	-2.34**	-0.31	0.62**	-2.02**	-2.18**

**. Correlation is significant at the 0.01 level (2-tailed).

851 **Table 3.** Correlation coefficient matrix among the chemical species for (a) winter, (b) spring,
852 (c) summer, and (d) autumn
853
854

(a) Winter

	MSA^-	Cl^-	NO_3^-	SO_4^{2-}	Na^+	NH_4^+	K^+	Ca^{2+}	Mg^{2+}	nss-SO_4^{2-}	nss-K^+	nss-Ca^{2+}
MSA^-	1											
Cl^-	-.199(*)	1										
NO_3^-	.365(**)	-0.166	1									
SO_4^{2-}	.481(**)	-0.125	.689(**)	1								
Na^+	-0.011	.876(**)	.209(*)	.261(**)	1							
NH_4^+	.562(**)	-.261(**)	.622(**)	.821(**)	0.081	1						
K^+	.446(**)	.281(**)	.568(**)	.759(**)	.561(**)	.744(**)	1					
Ca^{2+}	.303(**)	.347(**)	.513(**)	.478(**)	.524(**)	.372(**)	.533(**)	1				
Mg^{2+}	0.060	.848(**)	.240(**)	.291(**)	.966(**)	0.124	.589(**)	.545(**)	1			
nss-SO_4^{2-}	.496(**)	-.262(**)	.677(**)	.989(**)	0.116	.835(**)	.696(**)	.412(**)	0.153	1		
nss-K^+	.520(**)	-0.155	.518(**)	.748(**)	0.107	.829(**)	.879(**)	.338(**)	0.149	.755(**)	1	
nss-Ca^{2+}	.343(**)	0.052	.480(**)	.420(**)	.195(*)	.380(**)	.373(**)	.936(**)	.229(*)	.404(**)	.338(**)	1

855
856

(b) Spring

	MSA^-	Cl^-	NO_3^-	SO_4^{2-}	Na^+	NH_4^+	K^+	Ca^{2+}	Mg^{2+}	nss-SO_4^{2-}	nss-K^+	nss-Ca^{2+}
MSA^-	1											
Cl^-	.199(*)	1										
NO_3^-	.388(**)	.240(**)	1									
SO_4^{2-}	.349(**)	0.089	.619(**)	1								
Na^+	.258(**)	.888(**)	.418(**)	.467(**)	1							
NH_4^+	.368(**)	-0.150	.504(**)	.710(**)	0.026	1						
K^+	.305(**)	.416(**)	.703(**)	.710(**)	.639(**)	.474(**)	1					
Ca^{2+}	.236(**)	.353(**)	.665(**)	.485(**)	.355(**)	.258(**)	.516(**)	1				
Mg^{2+}	.382(**)	.872(**)	.519(**)	.416(**)	.912(**)	0.105	.660(**)	.545(**)	1			
nss-SO_4^{2-}	.418(**)	-0.008	.609(**)	.988(**)	.456(**)	.770(**)	.646(**)	.473(**)	.362(**)	1		
nss-K^+	.294(**)	-0.082	.539(**)	.578(**)	0.034	.631(**)	.655(**)	.360(**)	0.137	.611(**)	1	
nss-Ca^{2+}	.200(*)	.220(**)	.621(**)	.440(**)	.200(*)	.256(**)	.421(**)	.988(**)	.404(**)	.444(**)	.369(**)	1

857
858

(c) Summer

	MSA^-	Cl^-	NO_3^-	SO_4^{2-}	Na^+	NH_4^+	K^+	Ca^{2+}	Mg^{2+}	nss-SO_4^{2-}	nss-K^+	nss-Ca^{2+}
MSA^-	1											
Cl^-	-0.163	1										
NO_3^-	.422(**)	-0.161	1									
SO_4^{2-}	.425(**)	0.029	.376(**)	1								
Na^+	-0.065	.949(**)	-0.049	.192(*)	1							
NH_4^+	.359(**)	-0.243	.485(**)	.866(**)	-0.096	1						
K^+	0.123	.811(**)	0.062	.429(**)	.862(**)	.513(**)	1					
Ca^{2+}	0.127	.765(**)	0.148	.258(**)	.797(**)	0.195	.776(**)	1				
Mg^{2+}	-0.027	.939(**)	-0.009	.202(*)	.980(**)	-0.046	.885(**)	.817(**)	1			
nss-SO_4^{2-}	.535(**)	-.200(*)	.455(**)	.968(**)	-0.061	.911(**)	.242(**)	0.082	-0.039	1		
nss-K^+	.376(**)	-0.067	.471(**)	.666(**)	-0.007	.876(**)	.456(**)	0.212	0.053	.738(**)	1	
nss-Ca^{2+}	.277(**)	0.006	.259(**)	0.147	-0.016	.384(**)	0.151	.601(**)	0.045	.213(*)	.266(*)	1

859

860 **(d) Autumn**

	MSA^-	Cl^-	NO_3^-	SO_4^{2-}	Na^+	NH_4^+	K^+	Ca^{2+}	Mg^{2+}	nss-SO_4^{2-}	nss-K^+	nss-Ca^{2+}
MSA^-	1											
Cl^-	0.007	1										
NO_3^-	.517(**)	0.037	1									
SO_4^{2-}	.554(**)	0.104	.753(**)	1								
Na^+	.249(**)	.925(**)	.338(**)	.217(**)	1							
NH_4^+	.342(**)	-0.131	.360(**)	.463(**)	0.088	1						
K^+	.410(**)	.567(**)	.582(**)	.734(**)	.754(**)	.529(**)	1					
Ca^{2+}	.292(**)	.505(**)	.492(**)	.584(**)	.629(**)	.336(**)	.653(**)	1				
Mg^{2+}	.274(**)	.895(**)	.428(**)	.485(**)	.970(**)	0.122	.807(**)	.637(**)	1			
nss-SO_4^{2-}	.583(**)	-0.111	.760(**)	.970(**)	.224(**)	.610(**)	.626(**)	.483(**)	.310(**)	1		
nss-K^+	.359(**)	-0.137	.432(**)	.667(**)	0.189	.828(**)	.738(**)	.531(**)	0.230	.699(**)	1	
nss-Ca^{2+}	0.163	0.075	.364(**)	.442(**)	0.170	.477(**)	.343(**)	.879(**)	0.180	.434(**)	.623(**)	1

862 **. Correlation is significant at the 0.01 level (2-tailed).

863 *. Correlation is significant at the 0.05 level (2-tailed).

864

865 **Table 4.** Mean concentrations of major water-soluble species at Chichijima Island from
866 2001-2012 and those at several other remote marine locations in the Pacific
867

Location (data set)	NO_3^-	nss-SO_4^{2-}	MSA^-	References
		Present study		
Chichijima (2001-2012)	0.58±0.07	2.12±0.42	0.02±0.00	
		Other remote marine locations		
Fanning Island (1981-86)	0.16±0.08	0.67±0.27	0.04±0.01	Savoie et al., (1989)
Nauru	0.16±0.09			Savoie et al., (1989)
Funafuti	0.10±0.07			Savoie et al., (1989)
American Samoa (1983-87)	0.11±0.05	0.34±0.14	0.02±0.01	Savoie et al., (1989)
Rarotonga	0.12±0.08			Savoie et al., (1989)
Mid way (1981-2000)	0.29±0.16	0.56±0.45	0.02±0.01	Prospero and Savoie (2003)
N. Caledonia (1983-85)		0.42	0.02	Savoie and Prospero,1989

868

869

870

871

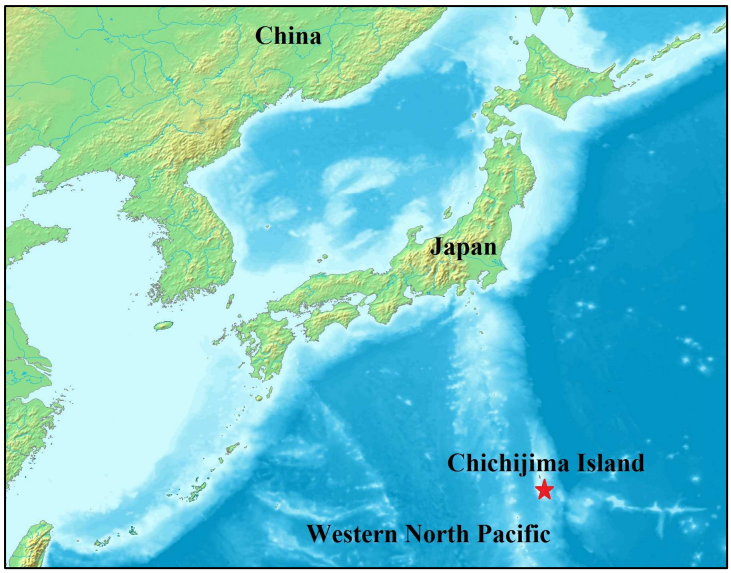

Figure 1. The geographical locationof Chichijima Island (indicated by red colored star) in the western North Pacific.

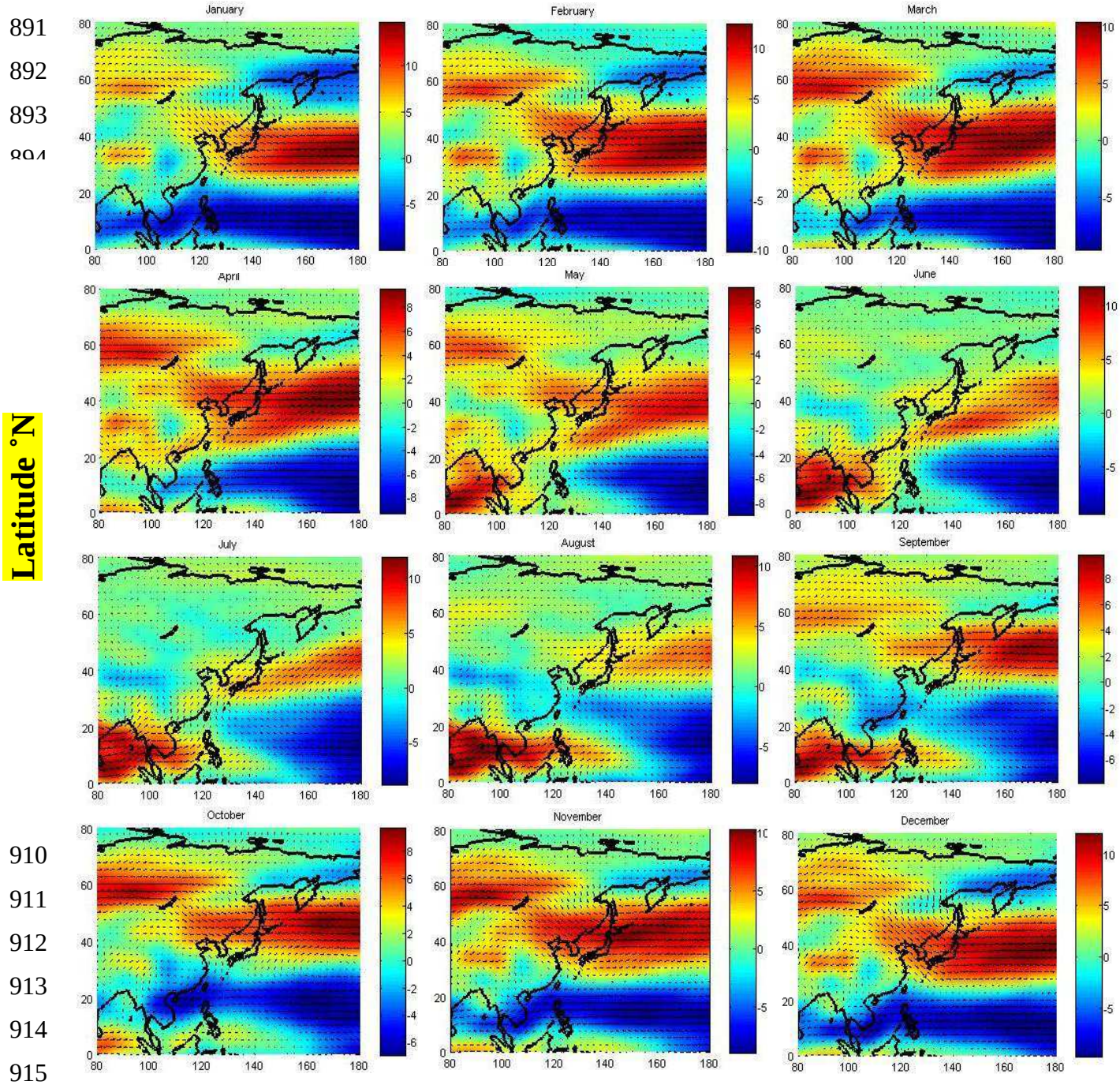

Figure 2. NCEP/NCAR reanalysis of Mean synoptic wind vector (m/s) at 850 mb pressure level for each month over the study area during 2001-2012.

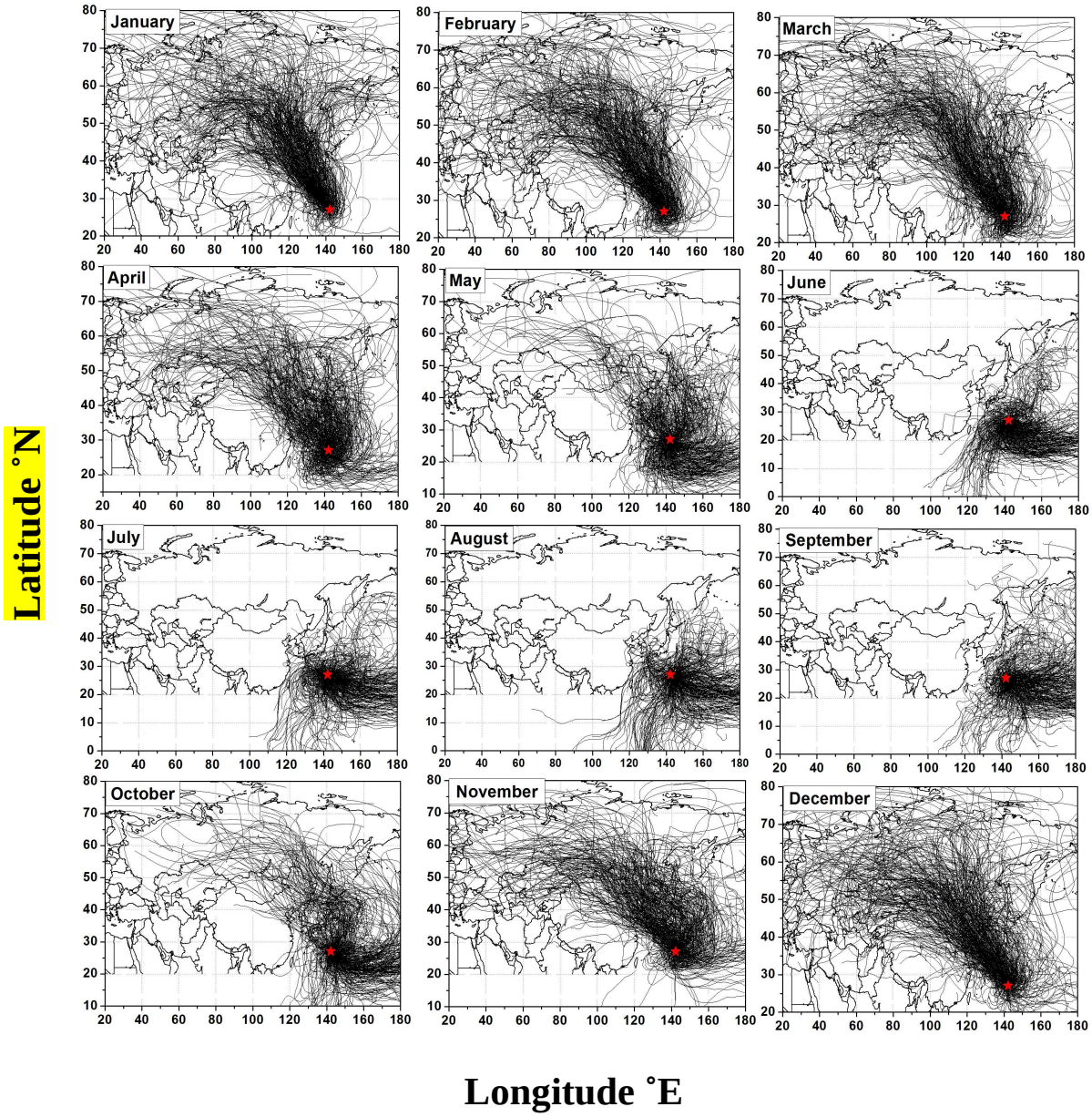

Figure 3. NOAA HYSPLIT 10-day backward air mass trajectories at 500 m a.g.l. for each month over Chichijima island during 2001-2012.

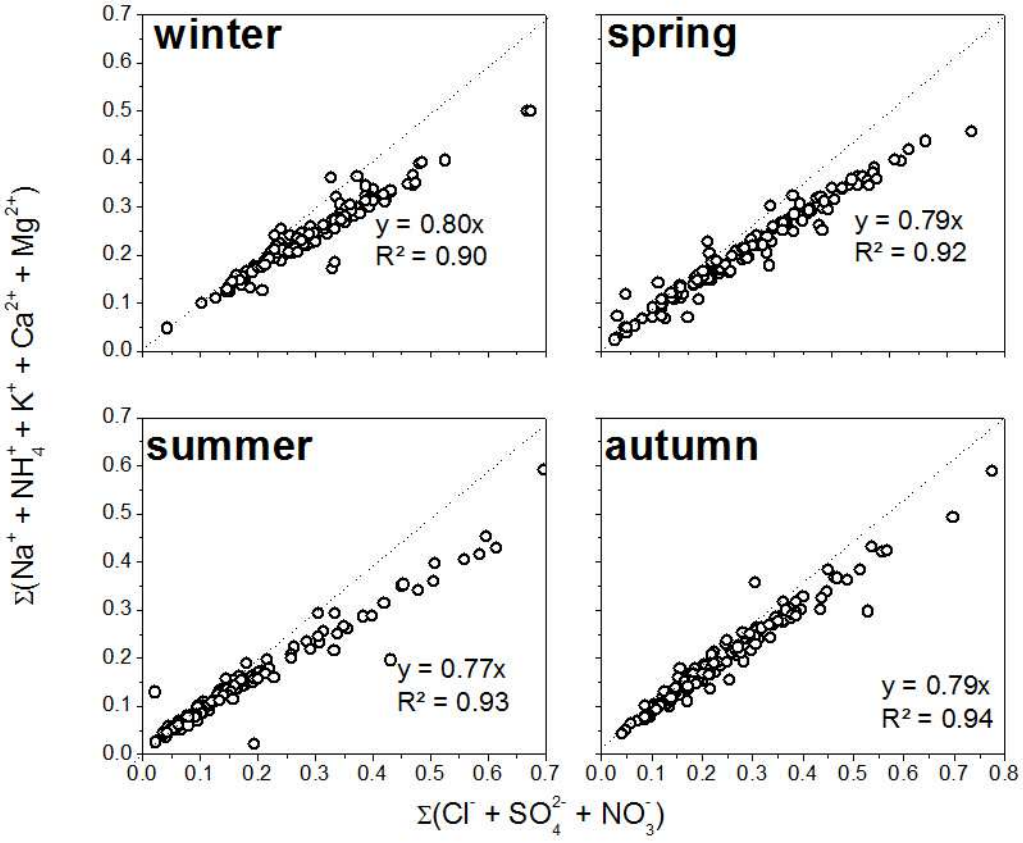

Figure 4. Charge balance of ions (μeq per m^3) on a seasonal scale.

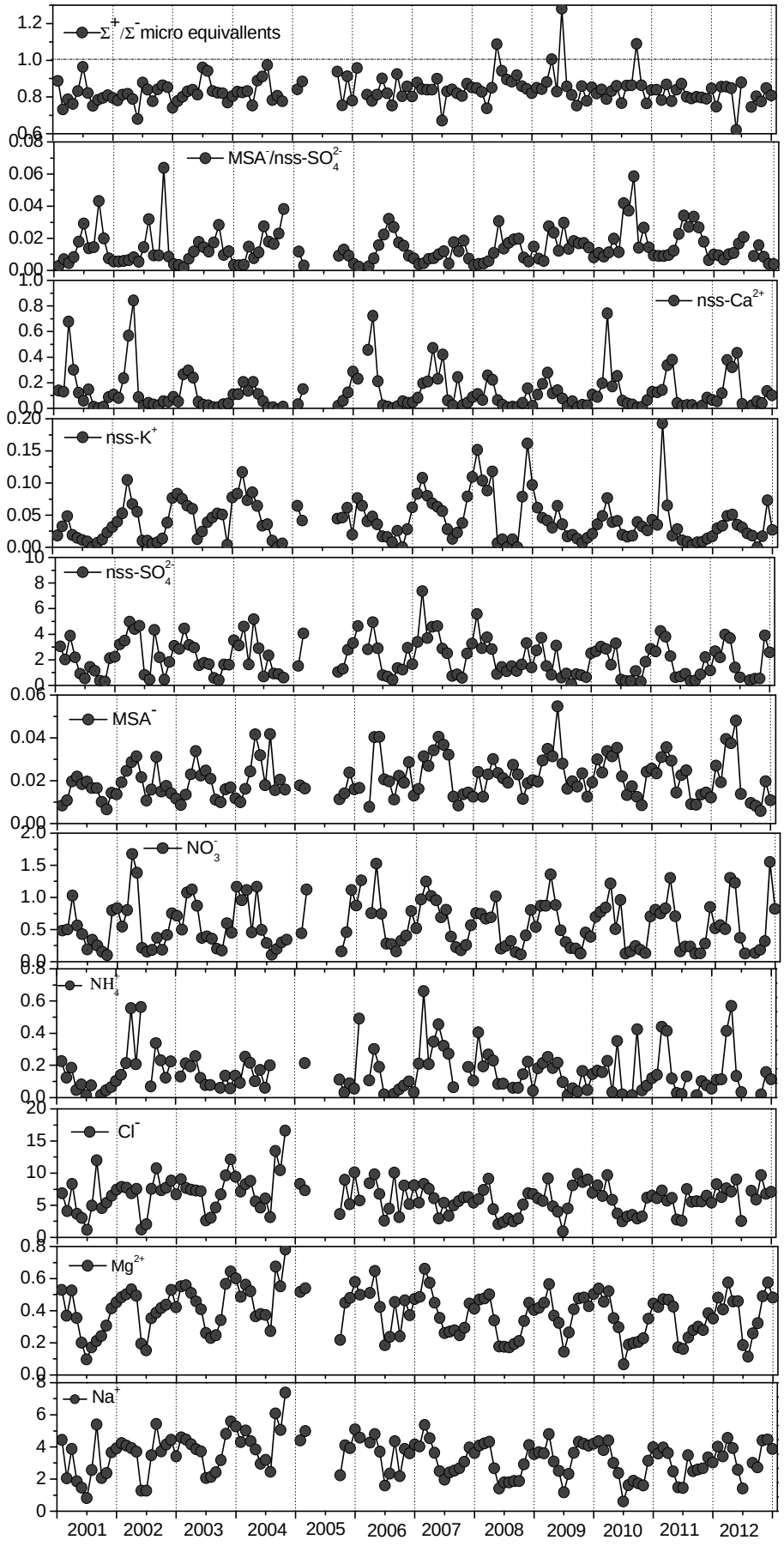

Figure 5. Temporal variations of different measured/derived inorganic ions (μg m^{-3}) and mass ratios over the western North Pacific during 2001-2012. Each data point represents one month in each year.

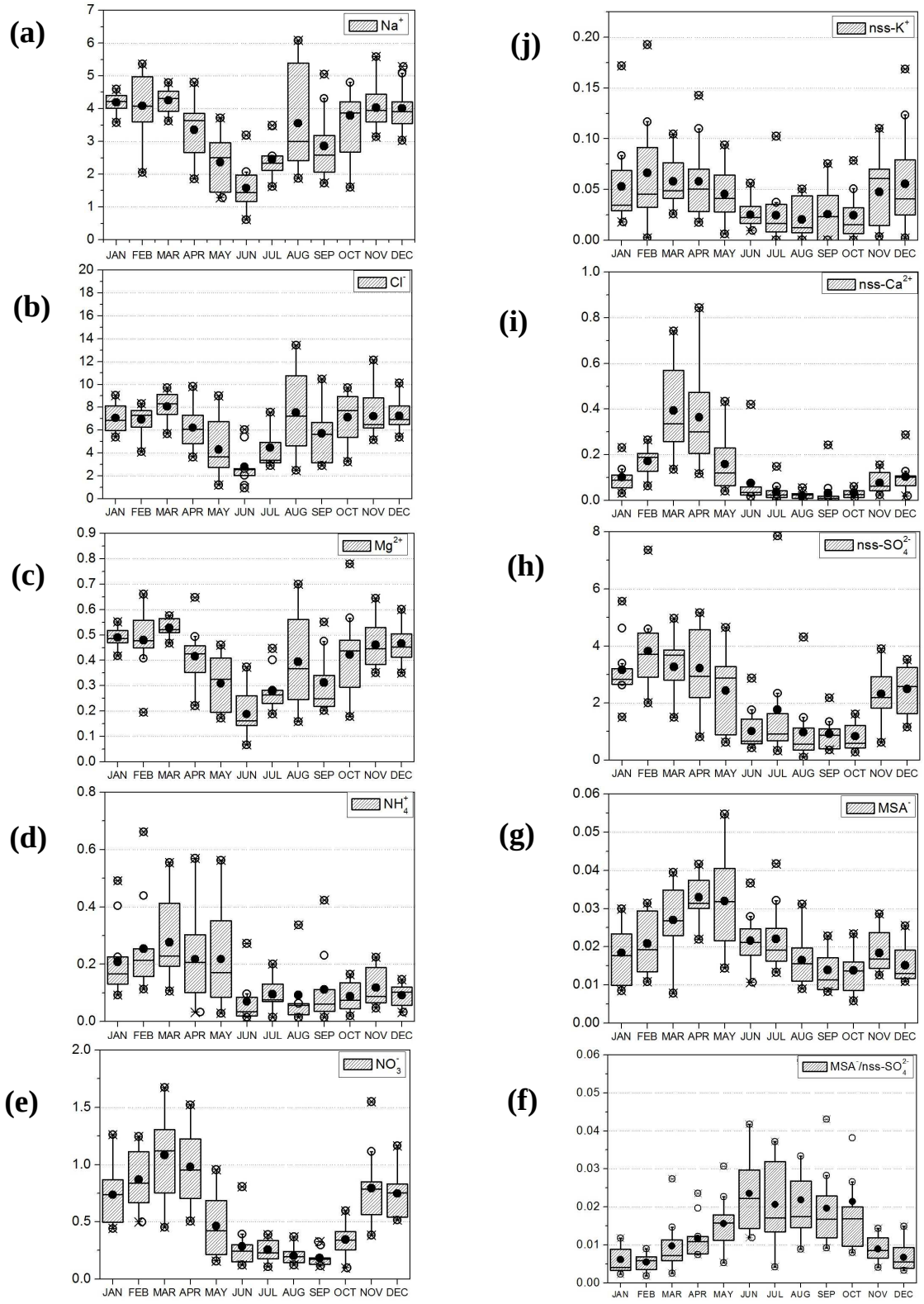

Figure 6. Box-Whisker plot of monthly variations of different measured/derived ionic species (μg m^{-3}) and mass ratio for the period 2001-2012 over the western North Pacific.

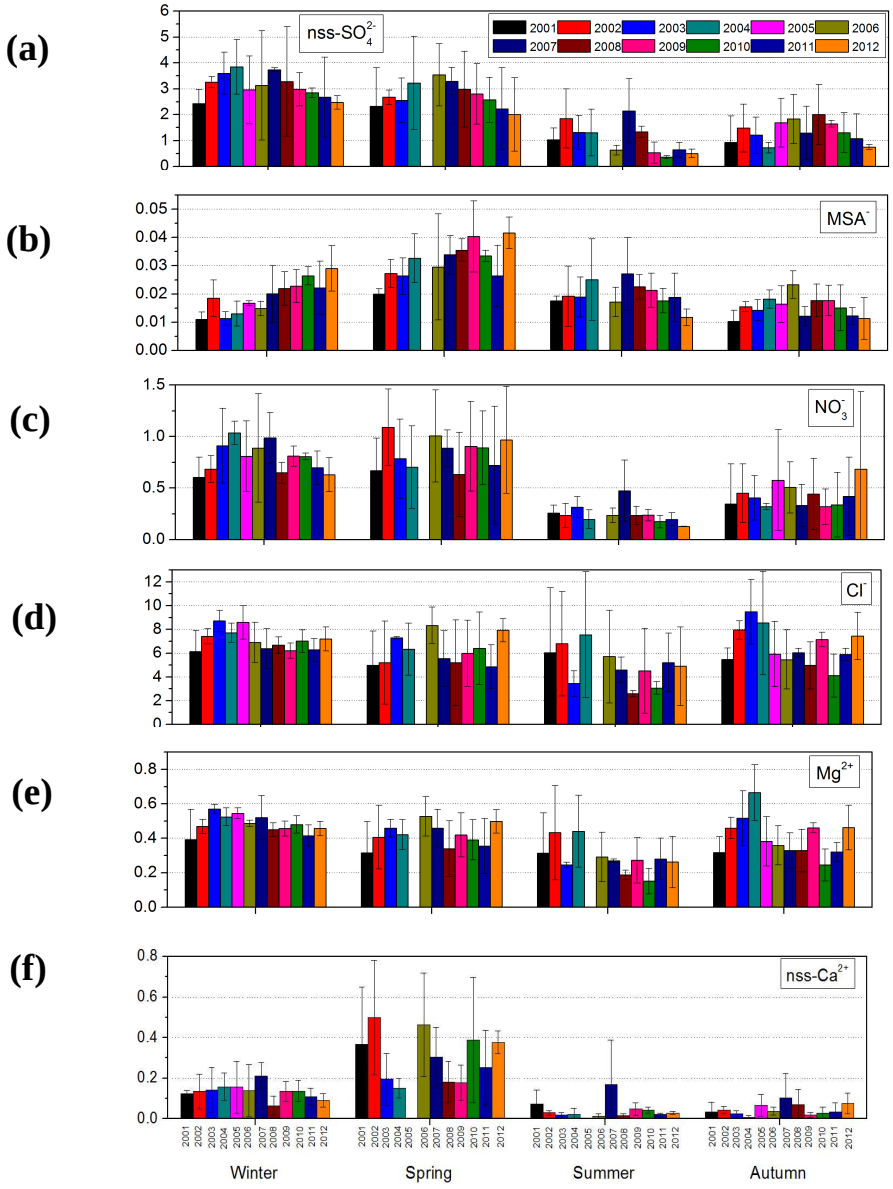

Figure 7. Annual variations of different chemical species (μg m^{-3}) on a seasonal scale over the sampling period of 2001-2012.

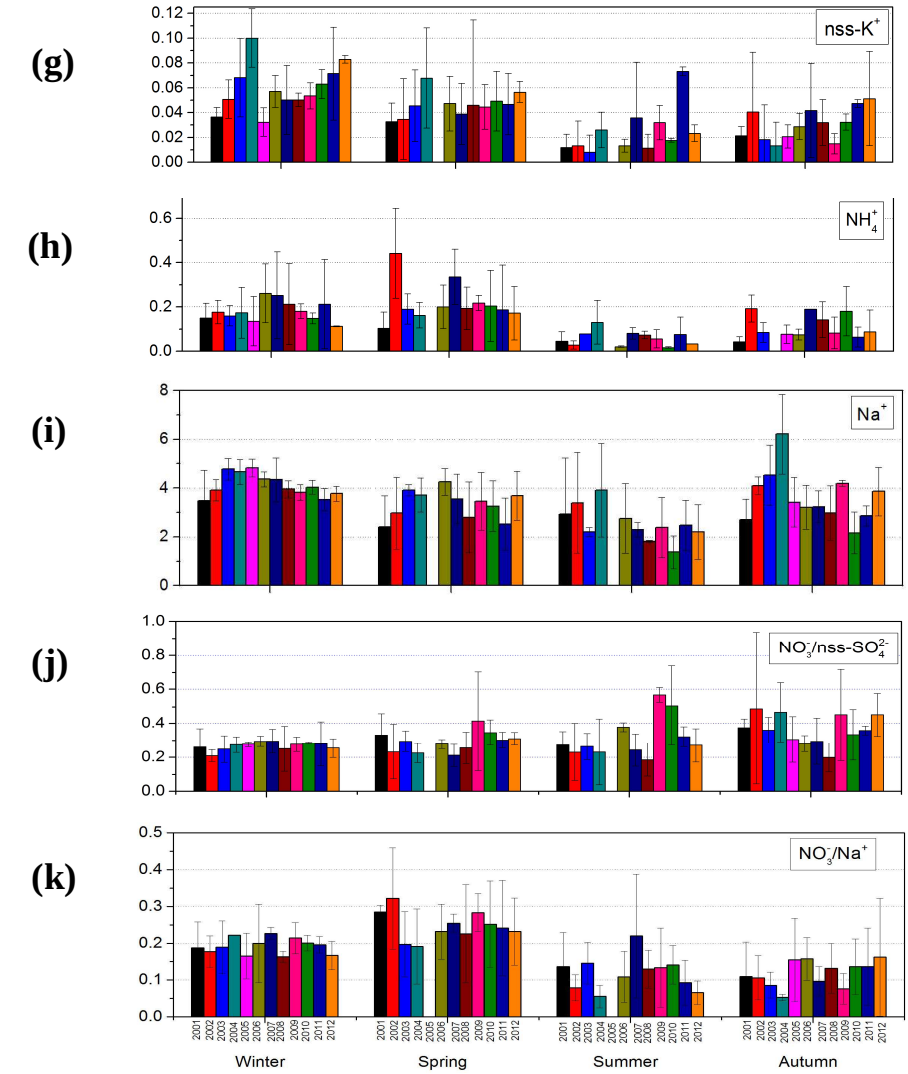

Figure 7. continued

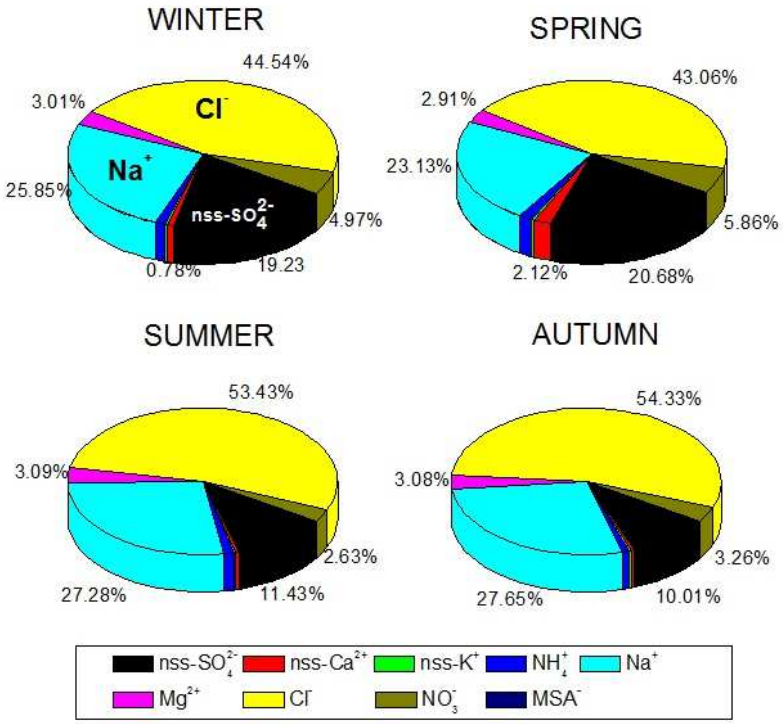

Figure 8. Percentage contribution of major ions to total water-soluble ions for different seasons.

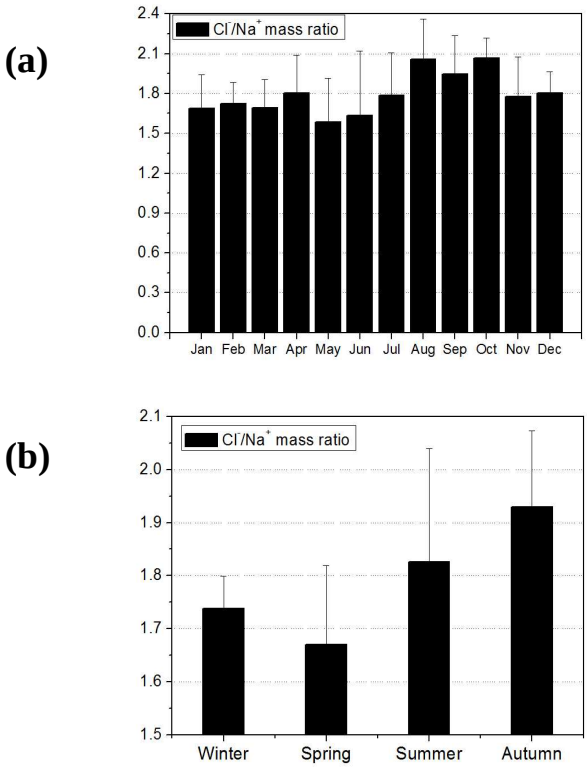

Figure 9. Variation of Cl^-/Na^+ mass ratio on (a) monthly (b) seasonal scales.

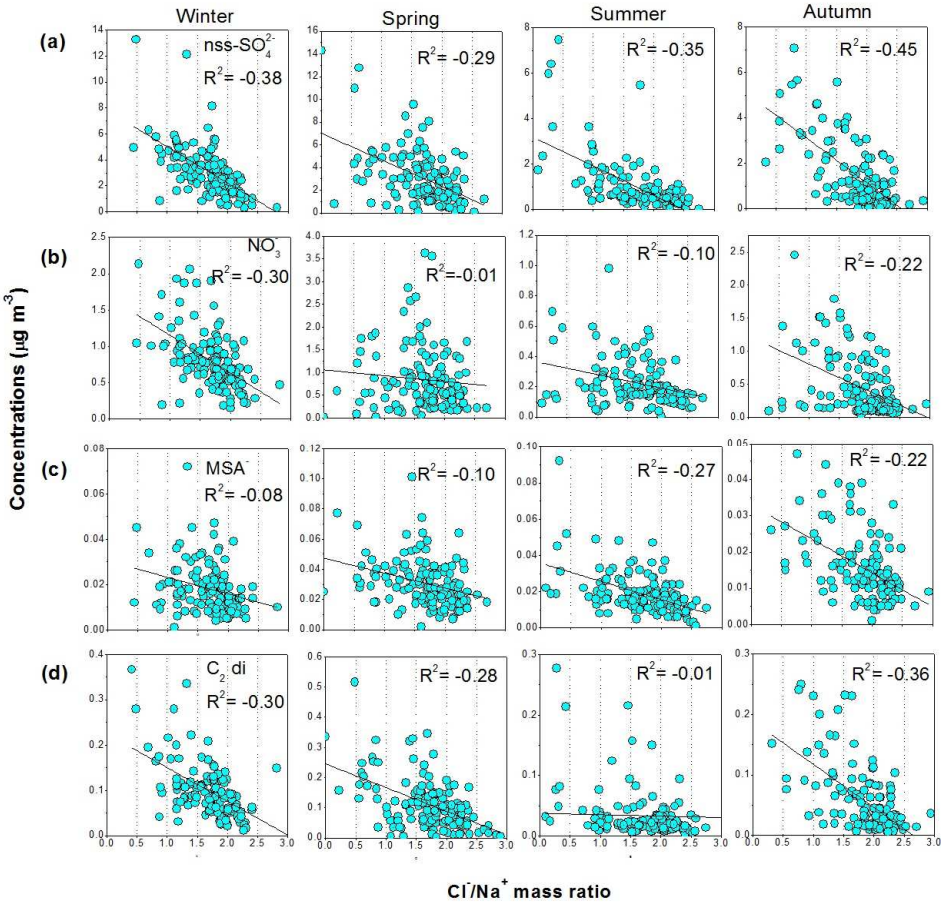

Figure 10. Relations between chloride depletion (Cl^-/Na^+ mass ratio) and acidic species (a) nss-SO_4^{2-}, (b) NO_3^-, (c) MSA^- and (d) oxalic acid (C_2di) for different seasons over the western North Pacific.

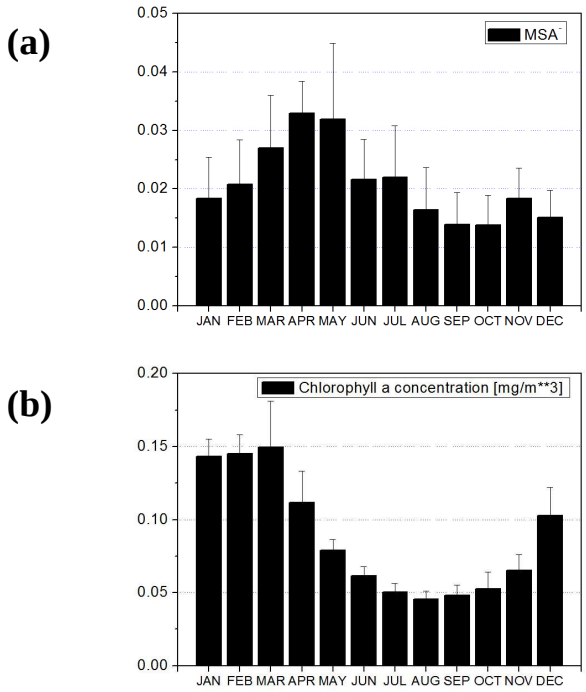

Figure 11. Monthly mean variation of (a) MSA^- (μg m^{-3}) (b) Chlorophyll *a* concentrations for the study period. Chlorophyll *a* concentrations were downloaded from MODIS AQUA satellite over the region (140E-145E, 25N-30N) for the study period.

1201

1202

1203

(a)

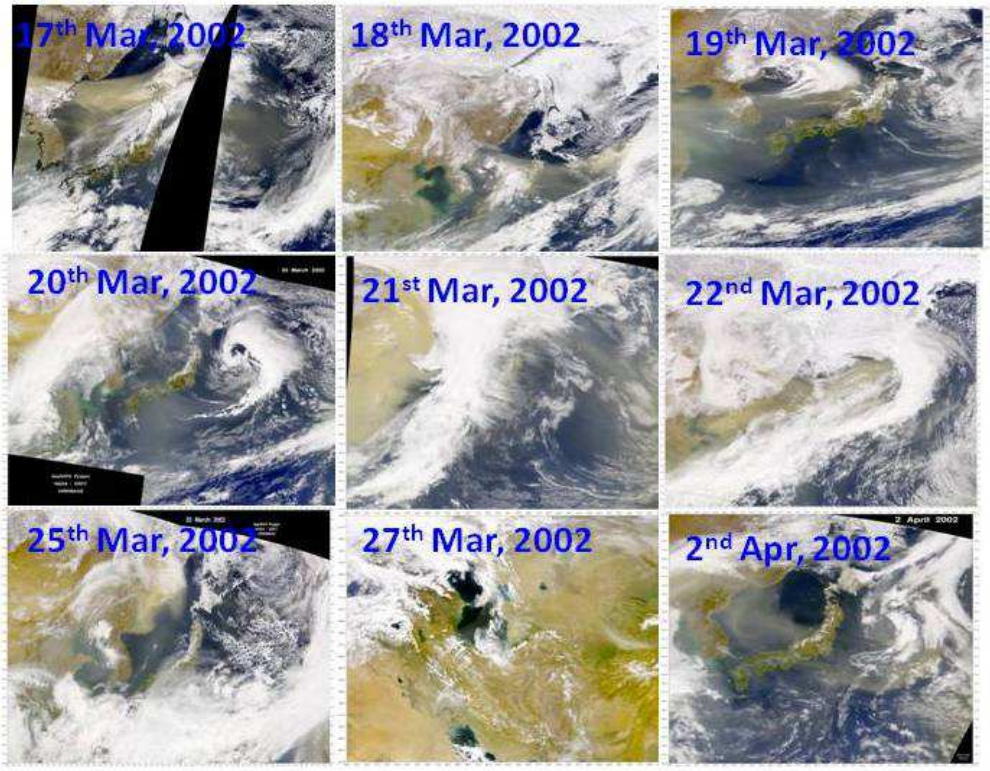

(b)

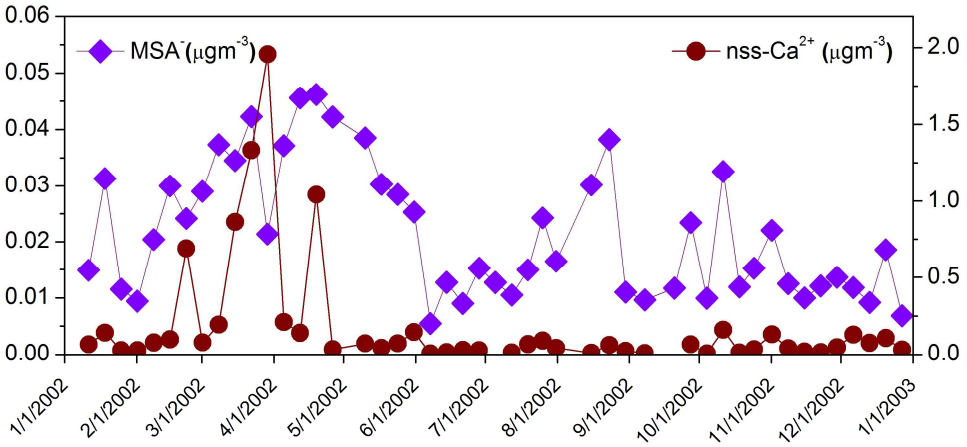

Figure 12. (a) The Sea-viewing Wide Field-of-view Sensor (SeaWiFS) images that captured the large Asian dust storm visible over the Sea of Japan and North Pacific during March 17-April 2, 2002 (b) temporal variations of MSA^- and nss-Ca^{2+} concentrations during 2002 over the western North Pacific. The black regions in Figure 12a are the gaps between consecutive SeaWiFS' viewing swaths and represent areas where no data were collected.